# Investigation of failure in different materials using acoustic emission technique

Submitted in partial fulfillment of the requirement for the award of degree of

**MASTER OF ENGINEERING**

IN

**CAD/CAM ENGINEERING**


*Submitted by*

**Kamaldeep Sharma**

Roll No. 801584014

Under the guidance of

**Dr. Sandeep Kumar Sharma**
Assistant Professor
Department of Mechanical Engineering
Thapar University, Patiala



**DEPARTMENT OF MECHANICAL ENGINEERING**

**Thapar University**

**Patiala-147004, India**



**July,2017**

# DECLARATION

I hereby declare that work done in this dissertation entitled, **"Investigation of Failure in Different Materials using Acoustic Emission Technique"** submitted towards partial fulfilment of requirement for award of **Master of Engineering degree** in **CAD/CAM Engineering** in **Department of Mechanical Engineering, Thapar University, Patiala,** is an authentic record of work carried out by me under the supervision and guidance of **Dr. Sandeep Kumar Sharma, Assistant Professor, Department of Mechanical Engineering, Thapar University, Patiala.**

This matter embodied in this report has not been submitted in part or full to any other university or institute for the award of any degree.

**DATE:** 01/08/2017

**Kamaldeep Sharma**

This is to certify that above declaration made by the student concerned is correct to the best of my knowledge and belief.

Sandeep Kumar Sharma
Assistant Professor
Department of Mechanical Engineering
Thapar University, Patiala

**Dedicated to**

**My parents and Friends**

# Acknowledgements

Through this, I would like to show my gratitude to all the great people who have an impactful influence on my life till now. It is all started during my Bachelor course, when I got familiar with an intellectual personality, **Dr. Jasmaninder Singh Grewal**, who taught me Solid Mechanics. His unique way of teaching, firstly, paved the way for me to ignite my interest for higher studies. Fortunately, in July 2015, I got the admission in Thapar University, Patiala with the discipline of CAD/CAM Engineering. After six months, I came across a very renowned personality in the domain of Structural Health Monitoring, named **Dr. Sandeep Kumar Sharma**. Eventually, I got the golden opportunity to work under his supervision.

I would like to acknowledge my mentor **Dr. Sandeep Kumar Sharma, Assistant Professor, Department of Mechanical Engineering, Thapar University, Patiala,** for his constructive suggestions and positive guidance in the thesis work. I would also like to show my deepest gratitude to **Dr. Shruti Sharma, Assistant Professor, Department of Civil Engineering, Thapar University, Patiala,** for her amiable support and providing quality knowledge regarding the topic **'Concretes'**. I am really grateful to spend many opportune moments under their outstanding management which inspired me a lot for carried out my research work.

Now, I would like to acknowledge **Mr. Ashutosh Sharma** and **Mrs. Shakshi Aneja, Research Scholar, Thapar University, Patiala,** who helped me at their best in programming section of my research work. At last, I would like to thanks all my friend who always backed up and motivated me throughout my complete research work, especially, **Mr. Jaspreet Singh, Mr. Gaurav Garg, Mr. Gaganpreet Singh Hunjan, Mr. Amardeep Singh, Mr. Baldeep Singh and Mr. Gurdeep Maan.**

**Kamaldeep Sharma**

# Abstract

To estimate the behaviour of different materials or structures regarding their inherent flaws and defects, there are different methods available within the domain of science and engineering. Nowadays, Non-destructive testing (NDT) is one of the most efficient method available for testing of any structure or equipment or part without damaging actual body of the specimen. Among the various NDT, wave based techniques are assuming importance since the propagation characteristics of the wave change with damage and can be directly related to the damage. Acoustic Emission (AE) technique is one of such passive wave based monitoring technique. Acoustic Emission waves are the elastic waves, generated by rapid release of energy from different sources like cracks initiation, propagation and growth. This technique is very much remarkably sensitive to crack advancement, able to grab the source of damage involves real time monitoring. Though with AE, various advantages exist for analyzing the true nature by localization of cracks within the material, however, there are still some shortcomings associated with AE data recording.

In this study, Acoustic emission technique was applied to track the damage progression under varying loading rates in different types of materials such as mild steel, concrete and FRP composites. Mild steel was loaded at 1.5, 4 & 8 mm/min, concrete was load at 0.5, 1 & 1.5 mm/min and FRP composites were loaded at 0.25, 0.5, 1, 1.5 & 2 mm/min. The AE data for mild steel and concrete was recorded using resonant frequency sensors R15α and R3α. For composites, Wideband frequency sensor WDI-AST sensor was used with a frequency range of 100-900 kHz.

The amplitude of AE hits and Ib-values analysis was used to quantify damage and to monitor the cracking patterns in all three materials. The recorded value of amplitude of AE hits were in total coherence with the load-time plot wherein major damage was indicated by higher values of amplitude. Ib-value analysis clearly indicated the damage severity in all the materials at all instants from moderate to severe. Ib-value also exhibited distinct curves for all the three materials. For mild steel, a major drop was observed during the yielding of the specimen and Ib-value remained constant for the rest of loading time. For concrete, there was a continuous fall in the Ib-value indicating that the damage was progressive leading to failure. For composites, the

fall was observed after half loading time indicating the damage progression only after certain extent of applied loading.

**Keywords:** Non-destructive testing, Acoustic emission, Sensors, Crack growth, Damage quantification, Improved b-value analysis

# Table of Contents

# List of Figures

# List of Tables

# List of Symbols

| | | |
|---|---|---|
| $M_L$ | = | Richter magnitude of the event |
| N | = | Number of events |
| a and b | = | Empirical constants |
| $A_{dB}$ | = | Peak amplitude |
| μ | = | Mean amplitude |
| $\alpha_1$ and $\alpha_2$ | = | Constants |
| σ | = | Standard deviation |
| A and n | = | Constant |
| ΔK | = | Stress intensity factor |
| N' | = | Count rate |
| $A_f$ | = | Amplitude at the location of sensing |
| $A_0$ | = | Initial amplitude at the location of sensing |
| $\alpha$ | = | Coefficient of attenuation |
| d | = | Distance travelled by the waveform |
| $V_{max}$ | = | Maximum voltage |

# List of Abbreviations

| | | |
|---|---|---|
| NDT | = | Non-destructive Testing |
| AE | = | Acoustic emission |
| AET | = | Acoustic emission technique |
| USA | = | United States of America |
| US | = | United states |
| Ib | = | Improved b |
| ASTM | = | American Society for Testing and Materials |
| PAC | = | Physical Acoustic Corporation |
| CITCO | = | Chandigarh Industrial and Tourism Development Corporation limited |
| UTM | = | Universal Testing Machine |

# Chapter 1.
# Introduction

## 1.1. Introduction to Non-Destructive Testing

There are a lot of techniques available to evaluate the behavior of the material and the non-destructive technique is one of them. In the non-destructive technique, damage in the material is identified without any cutting of material. There are so many non-destructive techniques are available to find the material behavior when it is subjected to change in its environment. Non-destructive testing is used to find out the characterization of damage and to identify the damage on the surface or inner without at a change in original structure or properties of a specimen. In other words, NDT is used to evaluate and inspection of components to find out the flaws, cracks or other damage with a comparison of some specific standards without cutting or any change in the shape or properties. NDT gives a cost-effective method to investigate individual specimen or can be applied to the whole specimen or a lot for investigation in a production quality control system [1]. These wide verities of NDT methods play significant roles in the investigation of composite materials, pipe and tube manufacturing, tank manufacturing, aerospace, military and defense, composites defect characterization and many other products. There are so many methods in NDT field to inspect the specimen like Ultrasonic testing, Visual testing, Acoustic emission testing, Electromagnetic testing, Liquid penetration method, Radiographic testing, Acoustic-Ultrasonic testing and many other methods are available[2].

Damage detection in the materials or NDT techniques can be divided into two types, one is passive approach and other is the active approach. The active approach needs excitation of checked (monitored) structure and then estimation of recorded responses or measurement of response. A number of techniques are developed in this area of non-destructive testing. For example ultrasonic testing, X-ray, vibration or modal analysis, etc. To detect the damage in composite materials, most of the time ultrasonic testing is used. Generally, these type of methods needs point by point measurements which result in high labor and time consuming when large size specimens are tested. For a plate-like structure which is large in size, guided ultrasonic technique is used to obtain on-line monitoring which results in less time and less labor work.

One and only major limitation of this technique is analysis and interpretation of waves due to their complex nature [3].

Passive approach does not need any type of actuation during damage detection process. In this approach, Transducers are used to monitor disturbance caused by rapid release of energy or heat due to an impact load, vibration etc. Acoustic Emission Techniques is the best example of this approach to detect the damage in structure or any other materials or specimens [3]. Details of the AE monitoring method is given in the following sectors:

## 1.2. Objective of Work

The main focus of this work is to evaluate the efficacy of Ib-value analysis to be able to define the intensity of damage in different kinds of materials (Mild steel, concrete and FRP composites). It is also utilized to understand the development of cracks and their progression in different materials.

## 1.3. Acoustic Emission Technique

Acoustic word is derived the form of the Greek word ‘acoustics’ which means ‘hearing’. So acoustic is something that is done with hearing. Many years ago, testing was done by the hearing the sounds which come from the structure before failure in the structure. For example, a branch of a tree during the break down it emits sound. Like visual inspection is done with eyes, acoustic emission testing is done with ears. So acoustic emission testing is done by hearing the sounds which come from the breaking of fiber when any type of crack grows or any other mode when any material or specimen goes under the stress [4].

### 1.3.1. Acoustic Emission Testing

AET (Acoustic emission testing) is a type of non-destructive testing which is used to find out defect and location of the defect in structure or component which is loaded or under any type of stress. AET generally provides all the knowledge about the flaws, cracks or any other defect in the structure means about the origin of crack or development of flaw (discontinuous) when the specimen is under continuous or repetitive stress. Any type of discontinuity or crack origin in the specimen releases energy and this energy travels in the form of high-frequency stress waves which are recorded with sensors [5]. These high-frequency waves are elastic waves by nature which arises from the quickly released energy from a crack or break down of fiber in the material. The range of acoustic emission frequency is 150-300 kHz more than normal audible

frequency. After recording the waves with sensors, sensor converts these waves into voltage. After that recorded data is analyzed and information about the source is extracted [6].

Generally, in this technology, ultrasonic sensors are used which listen to the sounds which come from the structure or material failure. A major reason for crack growth are hydrogen embrittlement, stress, corrosion, creep, fatigue, these can be identified by this technology. Leakage in high-pressure vessels can be also detected by this technology.

### 1.3.2. Brief history of the use of AE technology

Earlier in the history of acoustic emission, main efforts were directed at studying the behavior of materials during the deformation and probing the basic fundamentals of AE phenomenon and fracture of various materials. Modern day AE technique began in the 1950s in Germany and was made by Joseph Kaiser. He did his research work on the metals and discovered an effect which is known as Kaiser effect. According to the Kaiser effect, AE is not generated in a body until the previously applied load is not exceeded. AE term was firstly used by B.H. Schofield in 1954 in the USA. His report is published under entitle of Acoustic Emission under applied stress. After the basic theoretical study on the AE, it was applied in 1964 on the rocket-motor casing. After the successful testing of the casing, the technique was rapidly followed by many diverse areas like nuclear, petrochemical, construction industries and aerospace. In the 1970s the US federal highway administration did good no. of tests on bridges. More information about AE technique can be found in [7].

### 1.3.3. Acoustic Emission Sources

It is noted that the stress waves are produced by those cracks which are growing or active. No AE data will be recorded when the crack is present in material but it is not growing. Figure 1.1 given below shows AE setup.

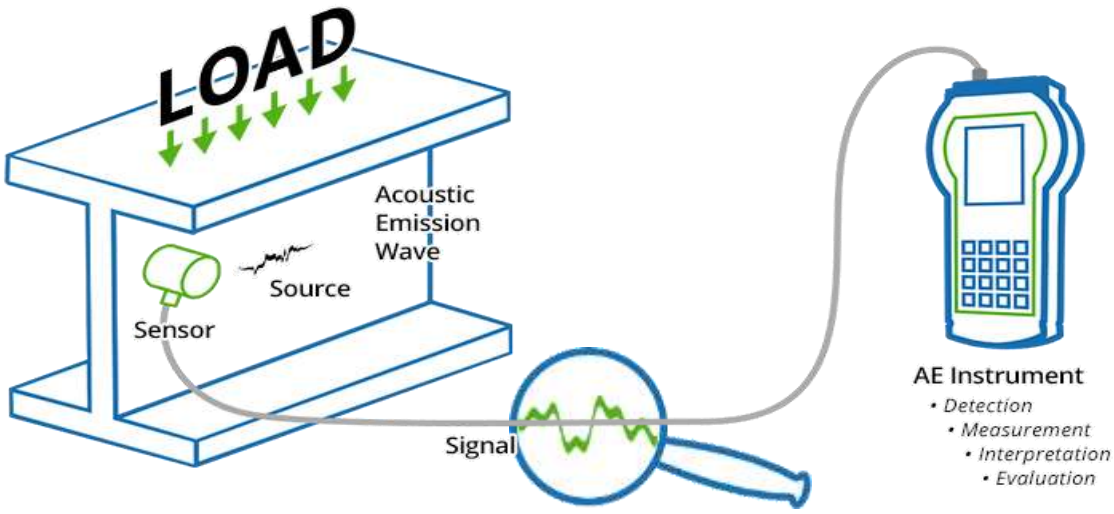


**Figure 1.1:** AE setup [W1]

Natural phenomenon earthquake can compare to the acoustic emission because, during the earthquake, seismic waves are released which are elastic waves in nature. Seismic waves propagate through the earth and are recorded by the no. of seismometers placed all around the earth. After the recording of seismic waves, data is analyzed and location and depth of source find out.

Many types of materials are inspected by AE. Some of them are –

- Wood
- Ceramics
- Polymers
- Rocks and geologic materials
- Metals
- Composites
- Concrete

Major sources of AE are –

- Fault slip (earthquake)
- Intergranular cracks
- Fatigue crack growths
- Fracture of inclusion particles
- Delamination in layered media
- Phase transformation
- Realignment of magnetic domains
- Slip and dislocation movement

- Rock bursts
- Fracture of reinforcement particles or fibres

### 1.3.4. Instrumentation for AE monitoring

AE setup consists many different parts like sensors, AE acquisition and analysis system, pre-amplifier shown in the figure 1.2 below:-

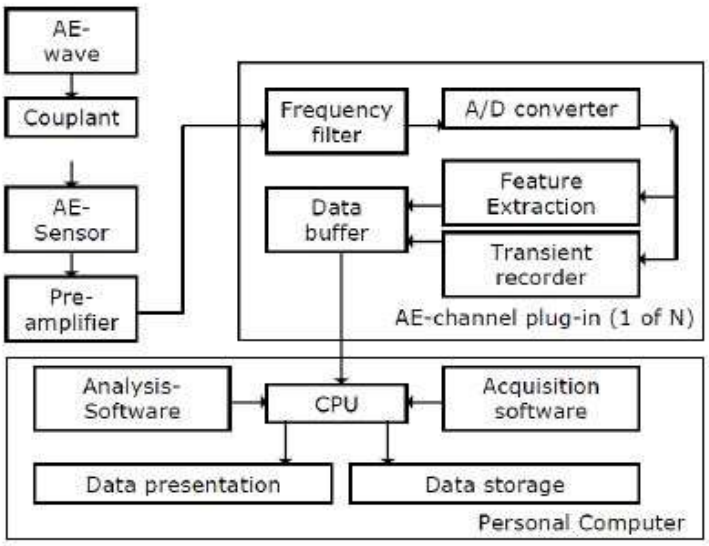


**Figure 1.2:** AE setup [19]

Waves are produced due to crack growth in the material. To record the waves or signals, with the help of couplant sensors are tied up with the structure or specimen. Different-different sizes and shapes are available for sensors shown in the figure 1.3:-

**Figure 1.3:** Variety of sensors [W2]

For efficient or effective transmission of AE signal waves, quality of couplant should be good. So that sensor will be placed as such that no major or minor signal will not be missed. For large size specimens, magnetic holding can be used to attach the sensors. For small or medium size

specimens glues, tapes and rubber band can be used which can hold the sensor tightly. As a couplant vacuum grease and oil is applied to the both surface i.e. one of the sensors and a second one of the specimen. During the selection of sensor operating frequency range is a major point to remember. For civil infrastructures, the frequency range is 100-300 kHz. Most of the times, during AE testing, piezoelectric sensors are used, which converts mechanical vibration into electrical signals. Piezoelectric sensors transfer 1 pm ($10^{-12}$m) elastic displacement into the 1μV electrical signal. On the base surface a wear plate is mounted and inside of the protective housing piezoelectric element is placed. A schematic of AE sensor is given below in the Figure 1.4.

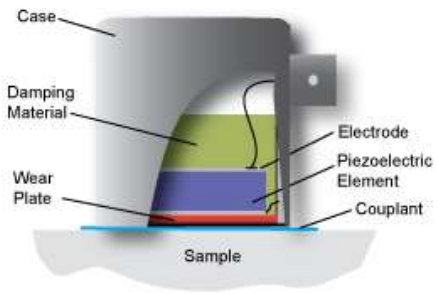


**Figure 1.4:** Sensor of the piezoelectric element [W2]

For effective testing, placement and selection of sensors are both important factors to find the damage.

Due to scattering, cracks, dispersion or conversation to another form of energy, AE waves amplitude decrease (which is known as attenuation). Attenuation is a major problem which puts the limit on placement of sensors because due to attenuation waves are able to propagate only up to some distance from the origin of defect or damage. Attenuation can be calculated by the under given formula:-

$$A_f = A_0 e^{-\alpha d} \quad (1.1)$$

Where $A_f$ is amplitude at the location of sensing, $A_0$ is initial amplitude at the location of sensing, $\alpha$ is coefficient of attenuation, d is distance travelled by the waveform.

Another constraint on the use of sensors is channeled in signal analyzing systems. Therefore carefully select the region where cracks are likely to occur, Sensors should be placed near to that region. After sensors, pre-amplifier is used because of signals generated during AE are often too small to detected so to amplify the signals, pre-amplifier is used before next step or processing. The range of amplification of the signal, signals are fed into AE data acquisition system and the

data is analyzed by using various acquisition and analysis software. To analysis, the data various tools is used.

### 1.3.5. AE Data Analysis Approaches

To analyze the data, basically, two approaches are there which are used.

I. Traditional approach i.e. Parametric based approach
II. Newer approach is Waveform based approach

Both approaches are discussed below.

**a) Parametric based approach**

In this approach, to gather the knowledge about damage or crack signal parameters are used. A basic AE signal is shown in figure 1.5 given below in which commonly used parameters are discussed below:-

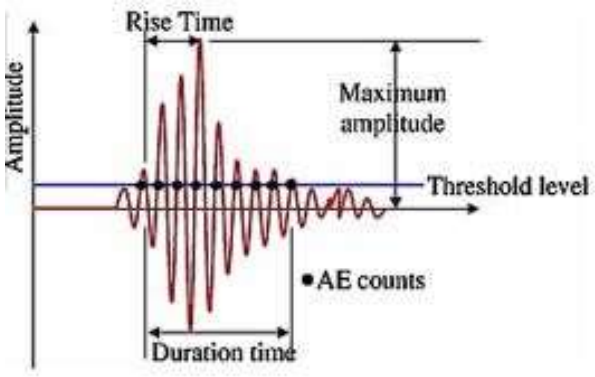


**Figure 1.5:** Parameters of AE signals [21]

**Threshold**: Recording is triggered once the output signals reach a set threshold value. This value is set to remove as much noise as possible, but care should be taken so that weak signals are not missed by setting the too high threshold.

**Hit**: A signal that exceeds the threshold and causes a system channel to accumulate data is known as a hit, thereby describing an AE event. Event rate is the number of events /hits per time.

**Amplitude**: Peak voltage of the signal waveform is a term of interest as it is closely related to the magnitude of the source event. The amplitude of the signals is expressed in volts or in AE decibel scale where 1μV at the sensor is defined as 0dB.

$$dB = 20 \log (V_{max}/1\ \mu V) - (\text{preamplifier gain in 1 dB}) \quad (1.2)$$

**Rise time**: Rise time is the interval between the time a signal is triggered and the time the signal reaches the maximum amplitude.

**Duration**: Duration is the interval between the time a signal is triggered and the time the signal decreases below the threshold value.

**Energy**: Energy of the signal is another parameter that conveys information about the strength of AE source. Various ways of expressing energy exist, such as area under the amplitude curve, RMS (root mean square) etc. energy as measured area under rectified signal envelope can be seen in figure 1.6. Absolute energy is derived from the integral of the squared voltage signal divided by the reference resistance over the duration of the AE waveform packet.

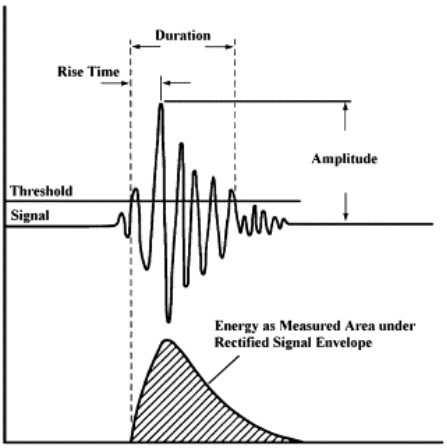


**Figure 1.6:** Energy as measure area under rectified signal envelope [22]

**Counts**: Counts are the number of times a signal crosses the threshold with the duration. In figure 1.5, one hit with five counts is seen. Count rate is also used regularly and denotes the number of counts per unit time.

To quantify an AE activity, a number of counts and number of hits can be used. The energy is sensitive to both amplitude and duration and operating frequencies and less dependent on the voltage threshold due to these reasons it is often used to interpret the magnitude of source event over counts.

Average frequency and RA are other useful parameters, which can be used to sort out the signals from shear cracks and tensile.

**b) Waveform based analysis**

As we know that in the parametric based analysis, discussed in the previous section, some parameters are recorded like hit, event, amplitude, energy but the signal itself is not recorded, which results in the fast recording of data and fewer data to analysis. But now when acoustic emission technique is fully or more developed, it is possible to record the full signal itself without any loss of data. Full data is recorded, so this approach (waveform based analysis) gives

better data analysis technique in compare to parametric based analysis approach. Because this technique allows the signal processing technique and in aiding in signal noise discrimination.

In this approach called waveform analysis approach, due to the nature of material and geometry of medium of propagation waveform is affected but the information about the source can be differentiated. By analysis of the waveform, information about the source can be expected and it also helps in differentiating the different sources of acoustic emission. The commonly used tool to analysis the recorded form is **frequency analysis** which is done by many methods like time-frequency analysis methods or Fourier transform such as short time Fourier transform & Wavelets frequency analysis can be done during the analysis of recorded data or when the data is being recorded because of fast computing ability is available.

AE signals are of two types basically which are generally seen: transient & continuous signals.

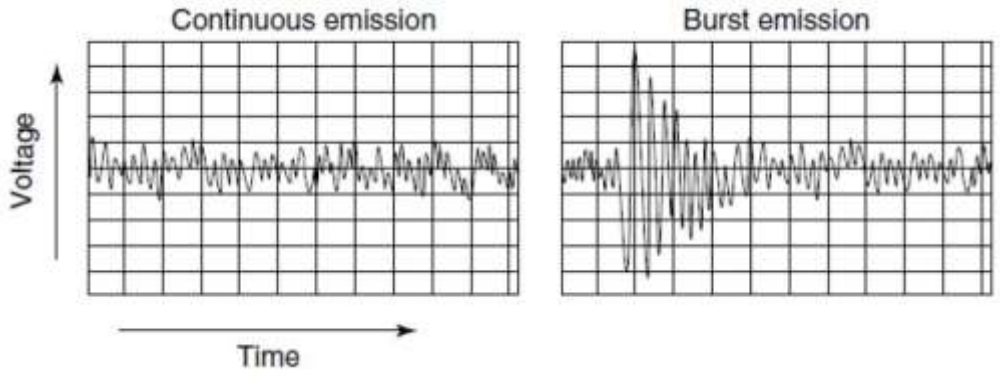


**Figure 1.7:** Continuous and Burst AE signals [23]

Transient signals occur only for short time interval and also called as bursts signals shown in Figure 1.7. Continuous signals occur for a long duration. It is noticed that the reason of burst signal is crack growth or fracture while continuous signals are noise signals. The major drawback of this signal is a generation of large data. The frequency range of AE waves can from few kHz to few MHz. To ensure the full data recording (without missing any major or minor signals) sampling rate should be at least double of the maximum frequency of the signals, according to the Nyquist criterion. Let the maximum frequency of the signal is 500 kHz, the sampling rate should be 1000 kHz. Despite this disadvantage, this approach is used widely due to the advantages offers in signal processing. Furthermore, AE waves travel in different modes and waveform based analysis is necessary to understand the modes of travel.

## 1.4. b-value Analysis

In order to assess severity, parameter that is used frequently is AE peak amplitude because AE is generated by most of source that have large peak amplitude. Attenuation rate of material is increased by collected damage because of cracks get scattered, which makes a signal of large amplitude attenuated even before being observed by sensor. This results in limited use of amplitude alone as it could result in errors. Therefore cumulative distribution is opted for studying amplitudes in a effective way because it has unique changes as accumulation of damage occurs.

Slope of the distribution falls with the evolving of damage which means the ratio of large & small energy AE events increases relative to total population of AE events. Therefore this technique of quantifying damage has turned out to be famous & is known as b-value analysis. Frequency of events with larger magnitude is less than that with smaller one and it is source for b-value analysis. This relation is defined as Gutenberg-Richter formula:

$$\log_{10} N = a - bM_L \tag{1.3}$$

Where $M_L$is Richter magnitude of the events, N is the number of events with magnitudes in the range $M_L \pm \Delta M/2$ and a and b are the empirical constants. The above formula is modified form which is used for AE technique and can be written as;

$$\log_{10} N = a - b'A_{dB} \tag{1.4}$$

Where $A_{dB}$ is peak amplitude of the AE events in decibels and can be expressed as:

$$A_{dB} = 10\ \log_{10} A_{max}^2 = 20 \log_{10} A_{max} \tag{1.5}$$

b value is then expressed as:

$$b = 20 \times b' \tag{1.6}$$

Thus b-value is the slope of the log-linear plot of frequency versus amplitude of AE events. It has been observed that during the change of stages, for example when the cracking is just started i.e. microcracks occur in the starting then b-value is high and it will be low when macrocracks will begin to occur. According to this fact, b-value is a likely candidate to judge damage progress.

## 1.5. Improved b-value (Ib value) analysis

Major problem with b value method is that most of time, amplitude of AE events versus distribution of frequency is not always linear. This it is necessary to have a modified analysis and

this new formula is known as improved b value analysis. In this method, statistical values of amplitude distribution (standard deviation and mean) are used. The Ib value can be expressed as:

$$Ib = \frac{\log_{10} N(\omega_1) - \log_{10} N(\omega_2)}{(\alpha_1 + \alpha_2)\sigma} \quad (1.7)$$

and

$$\omega_1 = \mu + \alpha_1\sigma, \omega_2 = \mu - \alpha_2\sigma \quad (1.8)$$

where μ is mean amplitude, $\alpha_1$ and $\alpha_2$ are constants and σ is standard deviation of amplitude distribution. By selecting the amplitude limits of the linear range of the cumulative frequency distribution data of AE, Ib value improves calculations. Ib-value is calculated for certain number of events ranging from 50 to 100 for better results during the test. In present study a group of 100 events with an overlap of 20 events are considered to calculate Ib-value. Ib-value for first 100 events is calculated then for 21 to 120 events and so on with an overlap of 20 events. A code has been developed to calculate Ib-values from the AE data recorded by the sensors during testing.

### 1.6. Advantages of AE Technique

Major advantages of AE technique over the other NDT technique are given below:

1. AE technique gives better sensitivity to crack growth than other techniques. It enables to detect the cracks in the early stages. It has been found enough sensitive to detect newly formed cracks on the surface up to few hundred square micrometers.
2. Small defects, occurring even in hard to reach or hidden areas are easily detectable by AE technique. Defects are detected as soon as signals can travel to the sensor. It is also possible to determine the approximate location of the crack using the times of arrival of signals from all the sensors.
3. It also enables real-time monitoring of the body or structure, as signals start as soon as crack occur. By recording the signals, it is also possible to provide the information about nature of the source.
4. It is also useable technique when it is not possible to interfere the normal activity of a body means without stopping the working of a body. Like during the inspection of nuclear plants, bridges, inspection can be done without stopping the reaction or traffic flow.
5. As mentioned above it is a passive technique, so no external energy is needed for testing, but the rising energy from the defect is utilized.

6. Although this is primarily used as a local technique to monitor a small distance of a structure, by increasing the number of sensors it is possible to use it for the complete structure or to monitor a larger area.

Basically, AE is different from other NDT techniques in two primary ways.

- It is a passive technique, no external source is needed for testing because signals originate due to cracks in the material itself.
- Second, AE detects movement while other methods detect geometrical discontinuities. The major difference between AE technique and other inspection methods are summarized in Table1.1.

**Table 1.1:** Characteristics of AE technique compared with other inspection methods[24]

| **Acoustic emission** | **Other methods** |
|---|---|
| Requires stress | Do not require stress |
| Detect movement of defects | Detect geometric form of defects |
| More material sensitive | Less material sensitive |
| Each loading is unique | Inspection is directly repeatable |
| Less geometry sensitive | More geometry sensitive |
| Requires access only at sensors | Requires access to the whole area of inspection |
| Less intrusive on process/plant | More intrusive on process/plant |
| Main problems: noise related | Main problems: geometry related |

## 1.7. Thesis outline

This present dissertation is organized as follows:

Chapter 1 has provided the introduction and background of AE technique, this chapter includes brief knowledge about the technique to analysis the recorded AE data and those techniques are used in this thesis work.

Chapter 2 has provided the literature review to gather the more information about AE technique, and concluding remarks of literature survey. It also consists objective of this work.

Chapter 3 presents experimental setup. In which experimental setup, used machines and details of used specimens are discussed. It also includes the details about AE setup which is used for AE monitoring.

Chapter 4 presents the results and discussion of testing. In this chapter, results are discussed for each material which was selected to do testing.

Chapter 5 includes the conclusion of thesis work and future scope of the work.

## 1.8. Concluding Remarks

In this chapter, AE technique is explained briefly. And it is concluded that AE has emerged as much used NDT technique. AE has lots of potential for accurate detection of damage. It offers various advantages over other NDT techniques but also has some limitations. AE has been applied successfully in every industry and a lot of researchers are contributing towards new modifications or applications in this technique.

# Chapter 2.
# Literature Review

## 2.1. Introduction

AET has recently been used by various researchers for non-destructive testing and monitoring. Few of the latest works done by using AET are discussed below:

**Kaphle *et al.*** [8] investigated damage quantification technique in acoustic emission monitoring. Authors used steel specimen of dimension 300mm×25mm×10mm. A notch was deliberately inserted in the specimen to initiate crack. INSTRON tensile testing machine was used for the loading rate of 2 mm/min. Three point bending was applied on the specimen. Two $R15\alpha$ sensors were mounted on the ends of the specimen for AE monitoring. The sensors were mounted with the help of grease and magnetic holders. The threshold was set at 60 dB after pencil lead break test. Loading was stopped after sixteen minutes. Ib was calculated for 50 and 75 events and the lowest Ib was found to be 0.7 about the time of 50s. The lower $Ib$ value is found in the yielding of specimen.

**Colombo *et al.*** [9] assessed damage of reinforced concrete beam using $b$ value analysis. The $b'$ value was calculated by multiplying b with 20. Author used 2.6 m long beam with a cross section of 125 mm $\times$ 270 mm. The beam was reinforced with 16 mm diameter deformed steel bar. The beam was simply supported with a span of 2 m and load was applied at two points. Load was applied in $5kN$ steps. Eight PAC R61 sensors were used. During the test the crack were classified with respect to the loading cycles. Cycle 1 had no cracks, cycle 2-5 involved cracks which were forming and the appearance of tensile crack along the span, cycle 6 involved appearance of shear cracks. The $b$ value was calculated as the slope of log-frequency- magnitude graph. It was found that lower $b$ value indicates macro crack whereas high $b$ value indicates micro cracks. b value greater than 1 and less than 1.2 indicates that channel was very near to large crack. b value greater than 1.2 and less than 1.7 indicated uniformly distributed cracks. $b$ value greater than 1.7 indicated macro cracks opening.

**Finalyson *et al.*** [10] explained the use of acoustic emission in aerospace field by monitoring health of an aerospace structure. Acoustic Emission Helicopter Health and Usage Monitoring System (AE-HUMS) was used to detect damage in helicopter drive trains. The test data obtained from SH-60 drive train was used to develop this system. It had made possible for finding a crack in pinion fifteen minutes prior to its failure. Damage was being characterized into four levels with the help of four colors - Green (no fault), Yellow (non-progressive minor damage), orange (definite and severe non progressive damage) and Red (severe progressive damage). Second technique was aircraft full scale fatigue test (FSFT). In this technique the actual fatigue spectrum which the structure faces during its flight, was taken into account. The objective of this test was to find fatigue affected regions and repair them in the prepared actual conditions.

**Wang *et al.*** [11] detected quality of friction welds using acoustic emission. Flywheel inertia type welding machine was taken for welding purpose. The welding machine was operated with hydraulic motor having speed of 4500 rpm. Dunegan/Endevco model 3000 system was used for acoustic analysis. Two sets of work piece were taken as shown in figure 2.1.

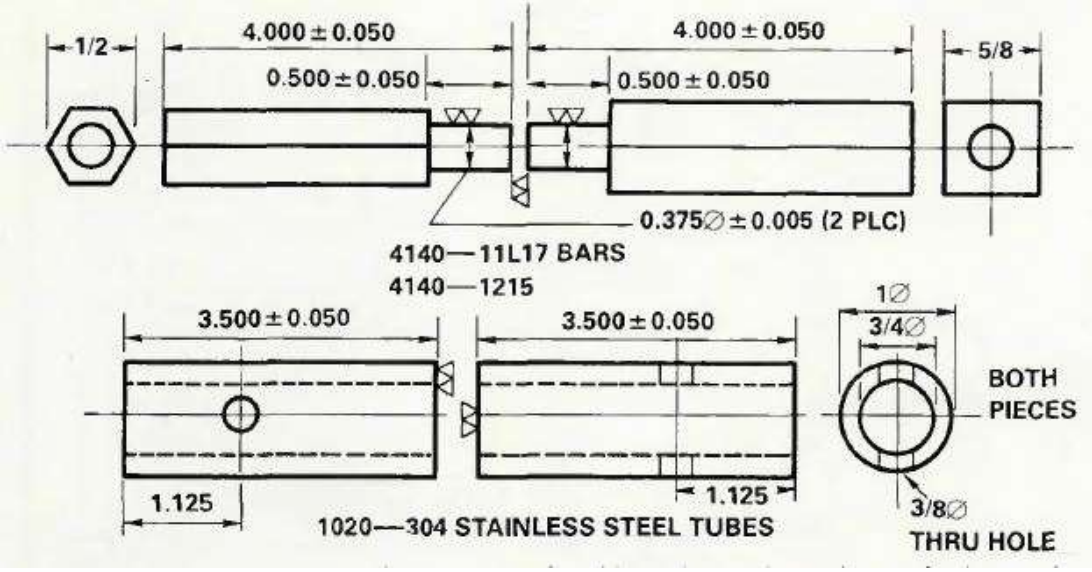


**Figure 2.1:** Specimens taken for welds

The hexagonal shape was taken to avoid slipping which could cause additional acoustic emissions. The square shape was taken so that sensors could be easily mounted. 200 samples were made. Six grades of carbon and alloy steel also were use$d$ to make work pieces keeping carbon content from 0.08% to 0.38%. Aluminum and copper also were introduced to have differentiation of events produced in ferrous and nonferrous material. Quenching experiments also were carried out on six ferrous and two nonferrous. Specimens were heated to $900^{o}C$ and

were quenched in air, water and oil to find the effect of different cooling rates. It was found that there were two distinctive burst of was acoustic emission in case of friction welding of ferrous metals. First *b*urst of AE occurred during welding and second burst occurred after completion of welding. First burst corresponded to the plastic deformation of metal whereas second burst corresponded to the martensitic transformation.

**Scruby *et al.*** [6] compiled the theory of acoustic emission. Events taken placed inside a solid material were picked by two or more sensors. Three application areas on the basis of source of high frequency sound were reported - process monitoring, structural testing, surveillance and material characterization. The source was a defect which radiates elastic waves as it grows along with monitoring of fabrication processes of various kind of materials. After this material research and development is included. The areas under which AE had come as a useful application were material degradation, reversible processes, leak and flow, fabrication Processes. As many processes had the tendency to generate acoustic signals but which had to be considered was the main issue. So researchers investigated that the localized spatial sources of sound which lie in normal bandwidth i.e. above 20 kHz were ultrasonic. In case of brittle crack high amplitude elastic waves carry a large portion of energy from the source. But in case of ductile crack the energy moved to drive dislocation in the enlarged plastic zone. Thus it helped in presenting the progress of crack. Instead of energy it was the energy release that controls the amplitude of AE signals. So the growth of brittle cracks should be readily detectable whereas slow ductile cracks were hardly detectable. In case of brittle materials, AE could be sensitive to very small increments in crack length($\approx 1\mu m$). In case of ductile materials AE could be insensitive to large crack advances.

**Drummond *et al.*** [12] studied emissions generated from wire ropes during proof load and fatigue testing. Authors used specimens that were made from 10mm steel wire ropes of a configuration of $6x36(\frac{14}{7}+\frac{\frac{7}{7}}{1})$ inner Wire Rope Core. This configuration consisted of a central king wire and other wires are wounded around it in helical form. The rope had a breaking load of $72.9kN$, a proof load of $25.5kN$ and a safe working load of $12.75kN$. Different damages were seeded in the wire with the help of saw. The acoustic transducers having sampling rate of 4 MHz and frequency band pass of 100 kHz-1.2 MHz (set by software) were employed to capture AE data. The acoustic emission signals having five or more than five counts were accepted. In the

initial stage proof load was applied several times on the undamaged rope and after that safe working load was applied three times. After that again proof load was applied. The damage was created then with the help of saw and safe working load was applied three times followed by final proof load. Threshold was taken as $40dB$. The qualitative and quantitative nature of the signals were explored and it was found that signals classily the condition of ropes while it is under periodic proof loading. It was found that signals above 80 $dB$ can differentiate between signals relating to damage and non-damage processes.

**Kurz *et al.*** [13] studied quantification of stress drop and stress distribution in concrete with the help of $b$ and $Ib$ value analysis. The ratio of weak events to strong events was denoted by $b$ value. In micro cracking a large number of AE signals were generated so it lead to a higher $b$ value. In of macro cracking $b$ value was lower. So as the stress increased $b$ value decreased from a case higher to a lower value as fracture process shifts from micro to macro cracking. Two parameters were needed in case of $b$ value analysis first being the event number and the magnitude of the event. Authors used beam with a cross section of $150 \times 150 \times 700$ mm$^3$. For reinforcement steel fiber of length 60 mm and of diameter 0.75 mm was introduced. A notch of depth 33 mm and width 3 mm was deliberately inserted in the middle of the beam. Servo hydraulic 100 kN test frame was used for the transmission of force using three cylinders. The lower supports were fixed and kept at a distance of 600mm. The third cylinder was kept in the middle at the top face. A static load of $7.5kN$ was applied. Eight sensors were used. The load was increased in the start, middle and end stage of the experiment.

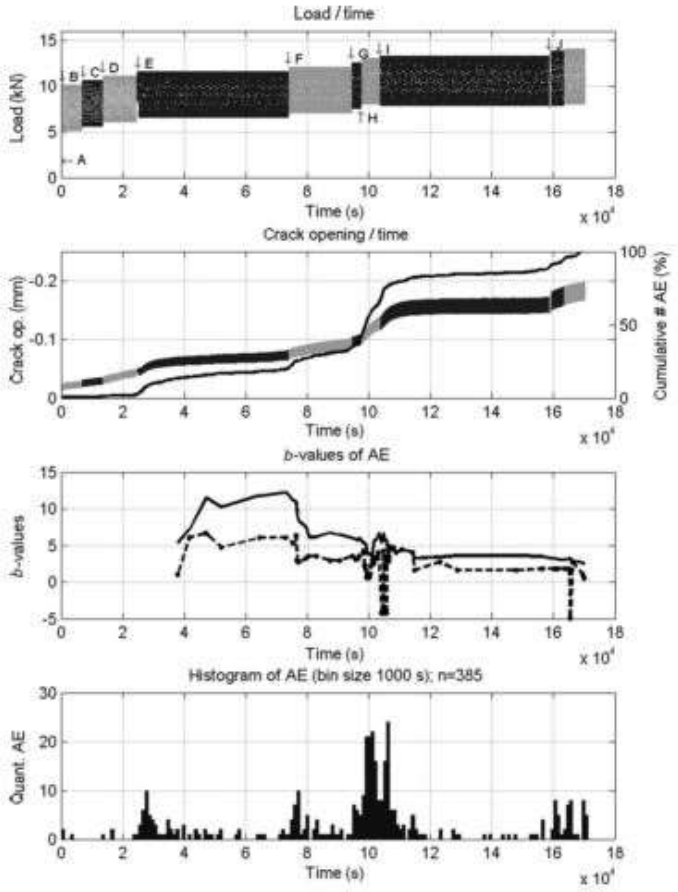


**Figure 2.2:** Variation of crack opening, b value and AE signals with time

The crack opening and equivalent AE were plotted with respect to time and it was found that they run parallel to each other thereby indicating that AE activity reflects crack opening. At the start of each loading phase it was found that a large AE signals were accumulated. The Ib curve had three large minima which coincided with the highest slopes on crack opening curve. It was found that b value was able to find fatigue in the material whereas Ib value gave occurrence of micro cracks.

**Loutas *et al.*** [14] compared the results obtained from single stage gearbox monitored with vibration based and AE based technique. Authors used a test rig with two gears ($045M15$ steel ) with pressure angle $20^0$, module 3 mm and have 25 and 53 teeth. Ball bearing were used to support shafts. Proper lubrication in the setup was ensured. Vibration based and acoustic based processes were applied to monitor gearbox. . The crack had been artificially induced in the gear. Bruel and Kjaer accelerometers were used in vibration based approach. Sampling frequency of 50 Hz was used and sign having duration of ls were recorded. Three sensors were used in AE

approach. These sensors were mounted on output shaft, bearing of the output shaft and with the input rotating gear. Various parameters from time and frequency domain were calculated for both testing methods. Parameter p1 denotes the mean of the signal, p5 is the absolute maximum of the signal, $p_4$ is the standard deviation of the signal, p6 and p7 are the third and fourth moments, p8-p11 results from the previous parameters are calculated by the signal in time domain. p12-p24 are calculated in time domain. In case of vibration based approach out of 50 parameters only 12 had the diagnostic potential. In vibration based approach p4, p6, p7, p12, p13, p17, p21, p24, ED1, ED2 and ED3 proved capable of attending the damage accumulation upon the gears. In AE approach p4, p6, p7, p12, p13, p17, p21, p24, ED3, ED4 and ED5 proved capable of attending the damage accumulation upon the gears. It was found that AE technique was more superior in the early and middle stages of crack propagation than vibration based monitoring technique.

**Proverbio *et al.*** [15] assessed damage in post tensioned concrete viaduct by *b* and Ib value analysis. Researchers reported that in brittle failure *b* value ranged ffom 1.5 to 2.5 in the initial stages then it decreased to 1. The *b* value was applied to a group of some events. 100 events were considered to calculate *b* value. To overcome this problem of making groups improved *b* value analysis was proposed. 13 and 8 span viaducts with span length of 22 m were built in 1956 on the national road number 114 on the eastern coast of Sicily island. A five cell longitudinal trapezoidal void section cross girder characterize each span Proof loading was applied for testing. In first loading cycle a 30 tons truck load was applied in the middle and 20 tons truck load was applied in the parallel line and then the truck was allowed to move. In second load cyde two 30 tons truck load was applied followed by 20 tons truck load on the parallel plane followed by 30 tons truck load in the same plane. The trucks were then allowed to leave. It was found that in first loading cycle, b value decreases with increase in load. In second loading cycle b value scatters. It was also found that Ib value was more sensitive in indicating changes in AE during microcrcaks and opening of cracks. During unloading the increase in the Ib value was related to shear crack mechanism.

**Haneef *et al.*** [16] studied tensile behaviour of AISI type 316 stainless steel using acoustic emission. The chemical compositions used to create specimens in terms of weight percentage were Cr/17.1, Ni/12.1, Mn/1.66, Mo/2.4, C/0.04, Si/0.67, Co/0.27, Cu/0.10 and Fe/Balance. Authors used specimens having dimension of 30 mm× 6mm × 5 mm annealed at 1273 *K* for 30

minutes. Specimens were subjected to tensile deformation at strain rates $1.4\times10^{-3}$ $s^{-1}$, $2.8\times10^{-3}$ $s^{-1}$, $6.9\times10^{-3}$ $s^{-1}$ and $1.4\times10^{-2}$ $s^{-1}$ at ambient temperature. Sensor having resonant frequency 150 kHz, preamplifier with 40dB gain and a band pass filter 100 kHz-300 kHz were used for AE monitoring. Threshold was set at 37dB. It was found that root mean square voltage of acoustic emission increases with increase in strain rate. AE dominant frequency increased with increase in strain rate as velocity of dislocation increases. During necking lower dominant frequencies were observed.

**Moustafapour *et al.*** [17] studied acoustic signals caused by the leakage in the gas pipe theoretically and experimentally. Leakage in buried gas pipe creating vibrations were theoretically analyzed and characteristics of AE signals were analysed. Authors used steel pipe of radius 130 mm, length 6m and thickness 6.4 mm. Two $R15a$ sensors were mounted on the top surface of the pipe for AE monitoring. An opening was created at a distance of 257.8 cm from one end of a pipe. The leakage was allowed through 0.6mm diameter hole. The pipe was buried in a contour of depth 50 cm and sand with a height of 5cm was poured on the pipe. Acquisition system with 16 channel was used. The sampling rate was set at 4 MHz. The operational frequency range was set at 50 to 500 kHz. To find the effect of surrounding medium the experiments were carried out with air-air and air-sand medium. Pipe was filled with air under pressure of 5 bar in both cases. It was found that maximum amplitude and power spectral density of waves was affected by the surrounding medium. In case of air as external medium these two factor have a larger value as compared to sand as surrounding medium. Maximum energy of signals were found near 120 kHz frequency.

**Sagar *et al.*** [18] studied the effect of loading rates on reinforced concrete with the help of b value analysis. At different loading rates the physical mechanism behind the behaviour of concrete under tension was summarized. A reinforced concrete beam was prepared with the dimensions shown in figure 2.3. Loading was applied through four point bending configuration.

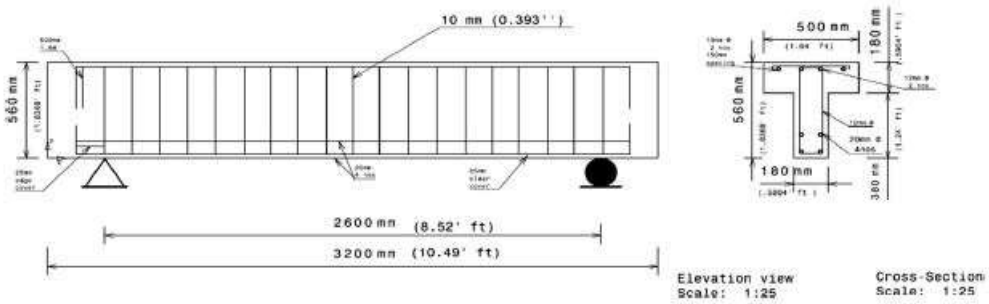


**Figure 2.3:** Concrete specimen dimensions

Distance of 1 m was taken as two point loading span and supporting span was kept at 2.6 m. A hydraulic frame of 1200 $kN$ was used along with acoustic emission setup. Loading rates of 4kN, 5kN and 6kN was applied. The variation of $b$ value with different loading rates is shown is figure 2.4.

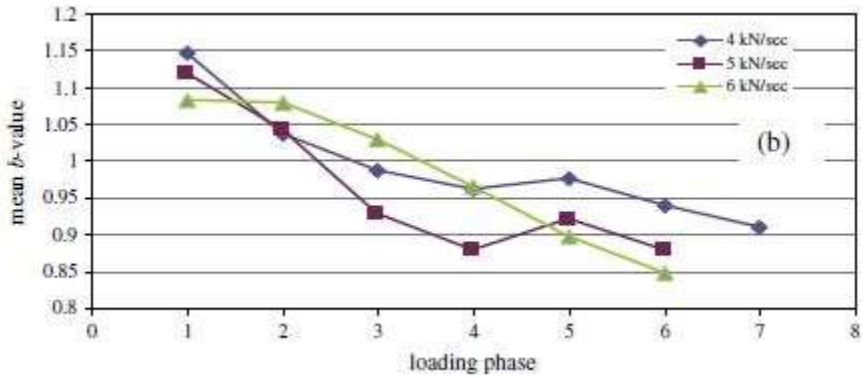


**Figure 2.4:** b value versus loading rate variation

It was found that with the increase in loading rate there was a drop in $b$ value. A sudden drop in $b$ value was found with the increase in RA value.

**Chen *et al.*** [19] analysed damage of FRP/Steel composite plates using acoustic emission. Index damage and modified index damage were calculated to analyse damage under cyclic uniaxial loading. Index damage was calculated by cumulative energy at any time divided by cumulative energy when the member experience maximum damage. It was hard to find cumulative energy at the time of maximum damage in practical applications so modified index damage had been proposed to overcome this limitation. Authors used four identical specimens of FRP/steel. The FRP was sandwiched between steel plates. The shape of the specimen is shown in figure 2.5.

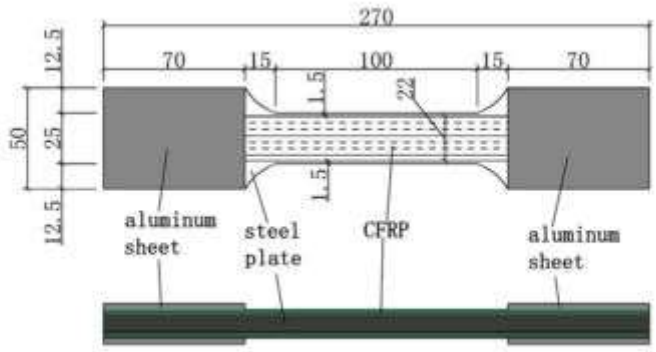


**Figure 2.5:** Specimen details

The specimens were tested on universal testing machine. AE sensor was mounted in the middle of the specimen for AE monitoring. The threshold was set at 40dB, main amplifier gain set at 20dB and preamplifier gain at 40dB. The filter frequency was set at 1 MHz. The rate of loading as set at 1mm/min. A sentry function was introduced to combine AE and mechanical information. It was defined as the natural logarithm of the ratio between mechanical (strain energy) energy and cumulative energy. It was found that AE energy is steady under uniaxial loading before failure. It was easily to find failure time through AE energy. It was also found that under cyclic uniaxial loading conditions cumulative AE energy increase faster in plastic stage than elastic stage. When index damage was 1 and modified index damage was 1.5 the specimen yields.

**Chuluunbat *et al.*** [20] studied influence of loading condition during tensile testing with the help of acoustic emission analysis. Authors used three specimen of aluminum alloy. Instron testing machine was used for tensile loading. Various strain rates $1.25\times10^{-4}$ $s^{-1}$, $2.5\times10^{-4}$ $s^{-1}$, $1.5\times10^{-4}$ $s^{-1}$ and $1.25\times10^{-3}$ $s^{-1}$ and $2.5\times10^{-3}$ $s^{-1}$ were applied on both plain and notched specimen. A 3 mm long and 0.3 mm wide notch was cut with the help of wire cutting. The crack propagation was recorded in the high speed camera. One general purpose wideband sensor was used. The tensile testing was carried out till fracture happened. The stress strain curve was divided into three regions first before the yield point, second between yield point and peak stress and third after peak stress. In case of notched specimen several hits were recorded in the first region. In second region small number of hits were observed. In third region AE activity was stable. The variation between parameters for notched and unnotched specimen is shown in figure 2.6.

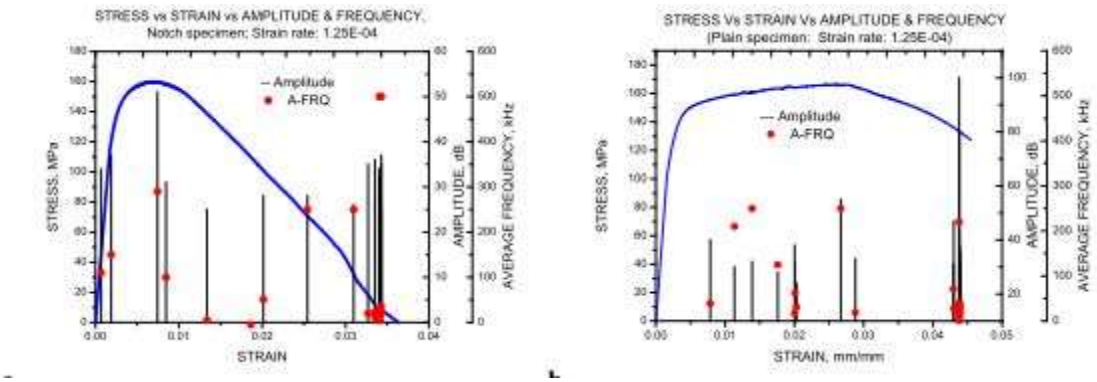


**Figure 2.6:** Variation among Parameters for notched and plane specimen [21]

Near the end of third region AE hit density increased leading to the fracture of specimen. It was found that in this region hits having amplitude up to 50dB and average frequency up to 500 kHz were present. During the testing of plain specimen it showed a different result than notched specimen. In the first region no AE was discovered. In the second region some AE hits appear indicating plastic deformation. Hits having high amplitude up to 50 dB and frequency up to 250 kHz were present. In the third region necking was observed followed by the final fracture generating a 100dB signal.

## 2.2. Concluding remarks

From this chapter, it can be concluded that acoustic emission has a potential to be used as a health monitoring tool for every type of structure. However it is a challenge to analysis of large volume data effectively created during testing. Nowadays instrumentation and sensors are well developed and it is quite easy to simplify the collected data. But how to manage the large volume of data to collect the important information is on the forefront of research.

# Chapter 3.

# Experimental setup

## 3.1. General

The objective of study is to compare the damage progression in different types of materials like mild steel (metallic and homogeneous), concrete and composite (Fiber reinforced polymers) (brittle and heterogeneous), using acoustic emission technique. A statistical analysis performed on recorded AE data, known as Ib-value analysis also known as Intensity analysis, is used to quantify the damage in the tested materials and also to distinguish the progression of damage in various kinds of materials.

## 3.2. Test Program

The test program and the methodology adopted for the study is as below and depicted in figure 3.1.

- Initially, the fabrication of different type of specimens, made of different materials of mild steel, composite and concrete is done in corresponds with ASTM and Indian standards respectively.
- Mild steel specimens of size 450 X 40 X 5 mm, are taken from previously fabricated steel plates, as per ASTM A370.
- Concrete samples are casted as per Indian standards 1026:2009 in cubes of 150X150X150 mm size for 28 days compressive strength testing.
- GFRP samples made as per ASTM D3039 having size of 250 x25 mm for tensile strength and were cut into the size 250 X 25 X0.8 mm.
- Two AE sensors was mounted on each specimen. For Mild steel, R15 α sensors were used. For concrete, R3 α sensors were used. For composite, WDI-AST sensors were used.
- The data is recorded and analysed (which results are mentioned in chapter 5). The load-time graphs are compared with AE signal intensity graphs to investigate the feasibility of AE monitoring.

- The failure progress and fracture of different types of materials is studied using AE technique. The crack initiation and propagation and its growth when these materials are tested in different types of strength tests is investigated and studied using AET.

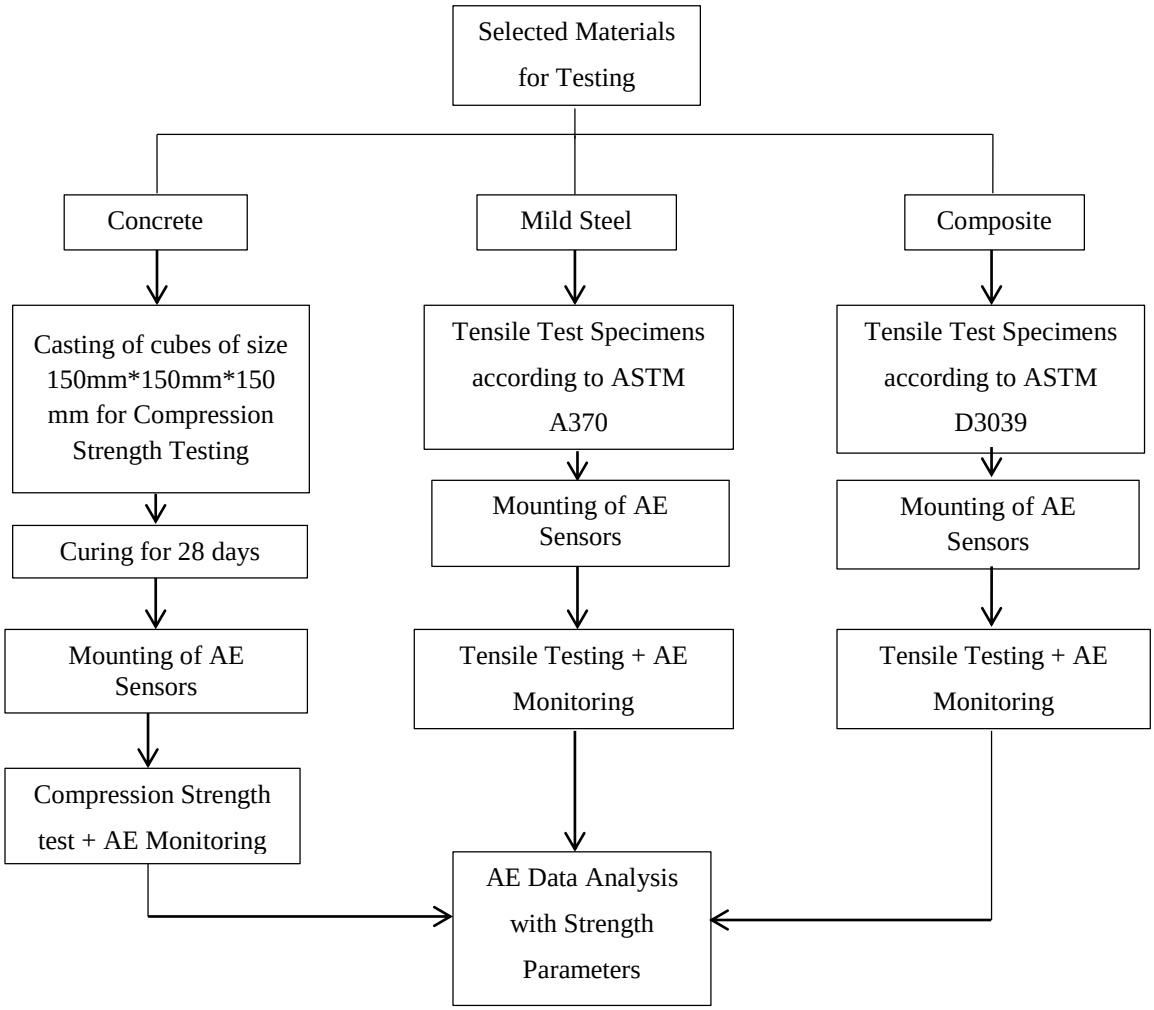


**Figure 3.1:** Methodology

## 3.3. Acoustic Emission Monitoring

Acoustic emission setup is installed to monitor crack progression and finally data was used for damage quantification. The equipment, discussed below, is used to capture AE data. The schematic of AE setup used in the study is generalized as below:

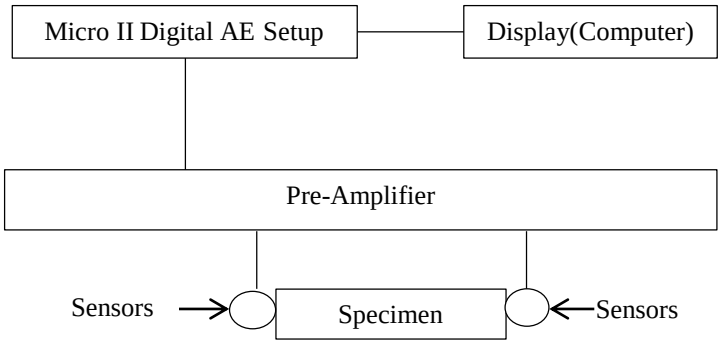


**Figure 3.2:** Schematic diagram of AE setup

### 3.3.1. Micro-II Digital AE System

AE data acquisition system, used in the present study, is Micro II Digital AE system provided by PAC MISTRAS GROUP shown in figure 3.3.


**Figure 3.3:** Data acquisition set up used for the study

It consists of 32 AE channels which means, in this system, up to 32 sensors can be used. It is directly connected to monitor. It includes a low power CPU, USB ports and integrated LEDs which gave indication of AE hits. It has its personal hard drive to save data.

### 3.3.2. AE Sensors

Since three different kinds of materials of entirely different properties are used. Three different kinds of AE sensors are used for AE monitoring of theses samples.

- **R15α sensor for Mild Steel**

R15α sensor is used to monitor the ductile material like mild steel used in this study. This is a general purpose sensor having high intensity and low frequency. It is used in various applications like vessels, bridges, pipelines, chemical plants as well as in applications related to factory and process monitoring. Figure 3.4 shows R15α sensor used in the study.


**Figure 3.4:** R15α sensor used for mild steel

The specifications of R15α sensor used in this study is given in table 3.1

**Table 3.1:** Specifications of sensor R15α

| S.No. | Specification | Value |
|---|---|---|
| 1 | Dimension | 0.75" dia. × 0.88" h |
| 2 | Weight | 34gram |
| 3 | Case Material | Stainless Steel |
| 4 | Face material | Ceramic |
| 5 | Operating Frequency Range | 50-400kHz |

- **R3α Sensor for Concrete**

R3α sensor is used to monitor the brittle material i.e. concrete cubes. This is general purpose sensor having low frequency, 30kHz resonant response. Thus, it is useful in those areas where low frequency is required by sensor for testing. This sensor is used in structural health monitoring of small concrete structures, metal pipeline leak detection and in areas where there is a need of high noise rejection. Figure 3.5 shows R3α sensor as another sensor used in this study.

**Figure 3.5:** R3α Sensor used for Concrete

The specifications of R3α sensors used in this study is given in Table 3.2

**Table 3.2: Specifications of sensor R3α**

| S.No. | Specifications | Value |
|---|---|---|
| 1 | Dimension | 19mm dia.× 22.4mm h |
| 2 | Weight | 43grams |
| 3 | Case Material | Stainless Steel |
| 4 | Face Material | Ceramic |
| 5 | Operating Frequency Range | 25-70kHz |
| 6 | Resonant Response | 30kHz |

- **WDI-AST Sensor for Composite**

WDI-AST sensor is used to monitor the composite material. Sensor is made up of piezoelectric material. Peak frequency of sensor is 292.97 kHz. Figure 3.6 shows the WDI-AST as third sensor used in this study.

**Figure 3.6:** WDI-AST sensors used for composite material

**Table 3.3:** Specifications of sensor WDI-AST

| S.No | Specifications | Value |
|---|---|---|
| 1. | Dimensions | 1.12mm dia.× 1.23mm h |
| 2. | Case Material | Stainless Steel |
| 3. | Base Material | Ceramic |
| 4. | Operating Frequency Range | 100-900kHz |

### 3.3.3. Preamplifier

It prepares an electric signal for further amplification. 2/4/6 type preamplifier is used in this study. It has an option of 20/40/60 dB gain. It operates with either signal ended or differential sensor. Figure 3.7 shows preamplifier used in the study.


**Figure 3.7:** Pre-amplifier

The major features of this preamplifier are

- 20/40/60 selectable gain.
- Low noise.
- Plug in filters.
- Input protection.

## 3.4. Material Selected

### 3.4.1. Ductile Material

As a ductile material, mild steel is used due to its daily life application in industries, construction and other places. It is having great features like easily availability, cheap and good damping property. Mild steel used for the study has following properties:

**Table 3.4:** Spectro analysis of used mild steel

| Nomenclature of sample | C<br>% | Mn<br>% | P<br>% | S<br>% | Si<br>% |
|---|---|---|---|---|---|
| Mild Steel sample | 0.1463 | 1.4430 | 0.01506 | 0.00352 | 0.3375 |

### 3.4.2. Brittle Material

As a brittle material concrete is chosen since it is the most commonly used construction material. It is very strong in compression and hence six cubes are casted in civil department of Thapar University, Patiala. Cubes of 150mm×150mm×150mm in size. Cubes are casted using guidelines of IS 1026:2009. The concrete mix was made in the preparation of 1:1.54:2.9 i.e. cement: sand: aggregate and water cement ratio is 0.5. Concrete mix is prepared using 43 grade O.P.C., two types of aggregate having 20mm and 10mm size with medium sized river sand.

### 3.4.3. Composite material

As a composite material fiber reinforced polymers (FRP) were used. Fiber reinforced polymers is a type of composite material which is made up of polymers and fibers are reinforced. In present study two types of FRP's are used, one is Glass fiber reinforced polymer (GFRP) and second one is Carbon fiber reinforced polymers (CFRP).

## 3.5. Ductile material - Mild Steel Testing

### 3.5.1. Specimen Details

Specimens are prepared by cutting the plate shape of steel, according to the ASTM A370 [25] . Shape and size of specimen is shown in Table. Figure 3.8 (a) and (b) shows the schematic and actual specimen details.

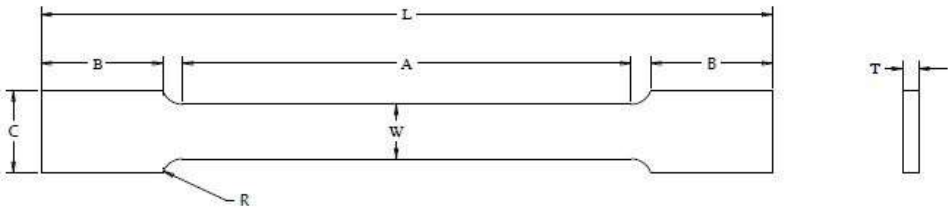


**(a)**

**(b)**

**Figure 3.8:** (a) Schematic of Specimen (b) Actual Specimen

**Table 3.5:** Dimensions of symbols used in the figure 4.6(a) are:

| Symbols | Meaning | Dimension (mm) |
|---|---|---|
| G | Gage length | 200±0.25 |
| W | Width | 400±3 |
| T | Thickness | 5 |
| R | Radius | 13 |
| L | Overall Length | 450 |
| A | Length of reduced section | 225 |
| B | Length of grip section | 75 |
| C | Width of grip section | 50 |

After cutting according to the requirement, with the help of sand paper, specimens are cleaned to remove the surface scale like rust. It would help in maintaining the proper contact between sensors and specimen.

### 3.5.2. Tensile Testing Details

For tensile testing of ductile material, UTM (Universal Testing Machine) was used which is placed in CITCO Chandigarh. Machine have capacity of 1000kN and is a hydraulic machine.

**Figure 3.9:** Mild steel Specimen during tensile testing mounted with AE sensors

Specimen was gripped between the jaws on UTM very carefully so that provided grip length on the specimen can be properly used. The data was recorded digitally by the equipment. Load was applied with different loading rates which are mentioned below:

**Table 3.6:** Nomenclature for mild steel

| **Specimens** | **Loading rates** |
|---|---|
| M1 and M2 | 1.5mm/min. |
| M3 and M4 | 4mm/min. |
| M5 and M6 | 8mm/min. |

During tensile testing, AE setup was also installed which is discussed in next section.

### 3.5.3. Acoustic Emission Testing

Two AE sensors of R15α were mounted on the surface of the specimen, for recording the AE data during testing, as shown in figure 3.10. The sensors were place at 90 mm distance from the center of the specimen on both sides. Both the sensors are mounted on the same face because thickness of specimen is less.

Preamplifier (explained in section 3.3.3) is used with gain of 40dB. The threshold value for recording AE data was preset as 40dB. This was done to exclude external noises such as machine noise etc.

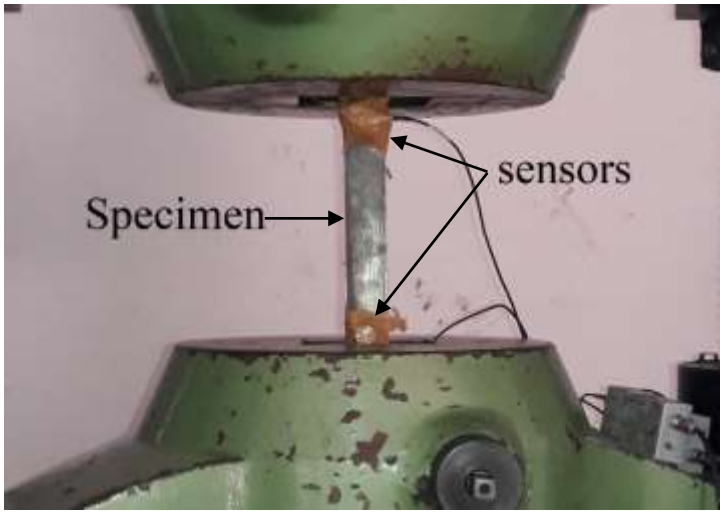


**Figure 3.10:** Mild steel specimen with mounted sensors

For effective transmission of AE signals, good contact of the sensors with test specimen is necessary. In this study sensors are attached on the specimen with the help of tape and as a couplant grease is used. The signals are amplified by preamplifier before recording in data acquisition system. Pencil lead break tests were performed to check if the sensors were mounted properly.

## 3.6. Brittle Material – Concrete Testing

### 3.6.1. Specimen Details

Concrete mix is prepared using 43 grade O.P.C., two types of aggregates 20mm and 10mm in size and medium sized river sand. The mix is designed according to the Indian standard 1029:2007.

In the present program, cubes are casted in mould of 150mm×150mm×150mm. Concrete mix is poured into the mould and using vibrator mix is settled with no air gap left. After 24 hours, cubes are removed from the mould and then cubes are cured in open water tank for 28 days.

### 3.6.2. Compression Testing Details

Compression testing was done on the same UTM which was used for tensile testing of mild steel. Cube was placed between the jaws. Lower jaw was fixed and upper jaw was moveable. Figure 3.11 shows specimen placed between the jaws.

**Figure 3.11:** Concrete Specimen during compression testing mounted with AE sensors

In this study, total six cubes are casted and compression test is performed on them. Three type of loading rates are used explained in Table 3.7. For each loading rate, two specimens are used to carry out the experiment and data was recorded digitally.

**Table 3.7:** Nomenclature for concrete

| Specimens | Loading rate |
|---|---|
| C1 and C2 | 0.5mm/min |
| C3 and C4 | 1.0mm/min |
| C5 and C6 | 1.5mm/min |

Due to load applied, deformation is occurring and cracks are growing. Cracks are emitting signals that are recorded by AE data acquisition setup.

### 3.6.3. Acoustic Emission testing

Sensors are attached to the surface of the specimen. During testing of concrete R3α is used explained in section 3.3.2(b). The sensors are mounted on the opposite faces of cube. One sensor

is mounted on front face and middle of face i.e. at 75 mm in x-direction and 75 mm in y-direction.

Preamplifier (explained in section 3.3.3.) is used with gain of 40dB. Threshold value is 35dB to avoid external noises.

A good contact of the sensors with test specimen is essential for effective transmission of AE signals. Sensors are kept in touch with the specimen, in this study, via tape wrapping and grease is used as couplant. Meanwhile, this study is going on, any acoustic phenomena within the specimen is tested and detected by the sensors. Thereafter, amplification of signals by preamplifier signals, before recording in data acquisition system, are amplified. Generation of AE signals are done by knocking which ensures the quality of signals detection.

## 3.7. Composite Material- Fiber reinforced Polymer Sheet

### 3.7.1. Specimen of Composite Material

Composite specimens are prepared according to the ASTM standard D3039 [26] i.e. length of 250 mm and width of 25 mm using a marble cutter. Average reading is taken for two samples. Two types of composites are used to perform tensile testing. Brief introduction to all composites types is given below:

1. Glass fiber reinforced polymer
2. Carbon fiber reinforced polymer

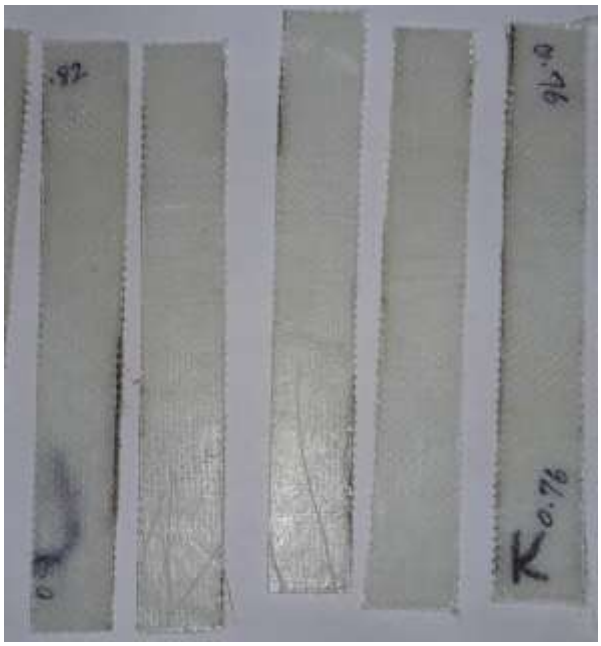

**Figure 3.12:** Composite specimens

### 3.7.2. Tensile Testing Details

For tensile testing of composite material, low capacity UTM was used which is placed in chemical department of Thapar university, Patiala. Zwick/Roell Z010 Universal testing machine was used and having capacity of 10kN, at different crosshead speeds. Figure shows the specimen holding on UTM.

**Figure 3.13:** Composite Specimen during tensile testing with sensors

In this study, 5 types of loading rates i.e. crosshead speed is used for samples. 2 samples are having same loading rates. Table 3.8 and 3.9 explains the loading rates which are used for testing

**Table 3.8:** Nomenclature for Glass fiber composite

| **Nomenclature** | **Loading rates** | **Material** |
|---|---|---|
| GF1 and GF2 | 0.25mm/min | GFRP |
| GF3 and GF4 | 0.5mm/min | GFRP |
| GF5 and GF6 | 1.0mm/min | GFRP |
| GF7 and GF8 | 1.5mm/min | GFRP |
| GF9 and GF10 | 2.0mm/min | GFRP |

**Table 3.9:** Nomenclature for Carbon fiber composite

| Nomenclature | Loading Rates | Material |
|---|---|---|
| CF1 and CF2 | 0.5mm/min | CFRP |
| CF3 and CF4 | 1.0mm/min | CFRP |
| CF5 and CF6 | 1.5mm/min | CFRP |

During testing, AE data is recorded in data acquisition system and further analysis has been done.

### 3.7.3 Acoustic Emission Testing

Again in this study, same setup is used. AE data acquisition system is micro II digital AE system provided by PAC (Physical Acoustics Corporation) MISTRAS GROUP.

Sensors are mounted on the surface of the specimen. During testing of mild steel WDI-AST is used explained in section 3.3.2(c). The difference between both sensors is 100mm. Both the sensors are mounted on the same face because thickness of specimen should be as less as shown in the figure 4.10.

Sensors are attached with the help of tape and grease is used as a couplant for proper contact between sensor and specimens. Threshold value is 30dB to avoid external noises. Figure shows the specimen while AE sensors were mounted.

**Figure 3.14:** AE sensors attached with composite specimen

## 3.8. Closing Remarks

In this chapter monitoring of common engineering material i.e. mild steel, concrete, composite using Acoustic Emission technique is discussed in detailed manner. Monitoring of crack growth in these materials projects a bright picture about failure of these materials.

# Chapter 4.

# Results and Discussions

## 4.1. Introduction

In this chapter, the results obtained from the acoustic emission testing of various engineering materials such as Concrete, Mild steel and Composites are analyzed. A tensile test was conducted on mild steel and composites (prepared in the lab), whereas concrete was tested under compression and, Acoustic emissions were recorded simultaneously. The focus of this chapter to investigate the efficacy of Acoustic emission technique to be able to track and estimate the quantity of damage undergone by the corresponding materials.

## 4.2. Tensile Testing of Mild Steel

The M.S. specimens were loaded in tension at three distinct strain rates of 1.5 mm/min, 4 mm/min and 8 mm/min as discussed in the previous chapter. The three strain rates were applied to understand the efficacy of acoustic emission to be able to pick variation of damage from slow to fast and to decide in which case, it performs better. Two AE sensors mounted on the flat surface of the mild steel bar were used to record data during the loading process. Further, the AE data was compared with the load-time data obtained from the UTM in an attempt to study the damage progression in the material. For damage quantification, AE intensity analysis including the analysis of amplitude of AE hits and a specific statically analysis of amplitude of AE hits known as 'Ib-value analysis'. The results are discussed in three parts as per the strain rates used.

### 4.2.1. M1 and M2 Specimens at 1.5 mm/min rate of loading

Two MS specimens (M1 & M2) were subjected to a strain rate of 1.5 mm/min was to ensure repeatability of acoustic emission data analysis and the results were obtained from both UTM and acoustic emission setup. The best of two plots was selected for analysis.

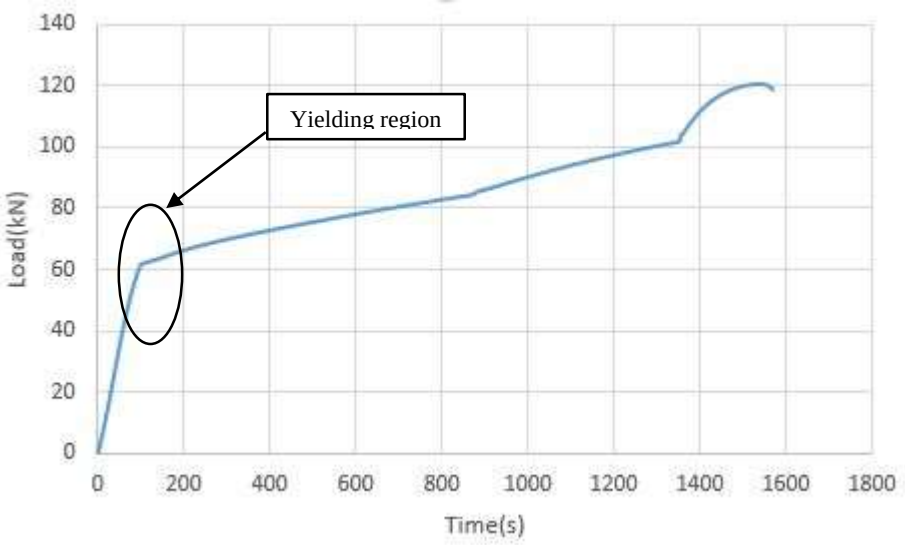


**Figure 4.1:** Load vs Time graph for mild steel specimen

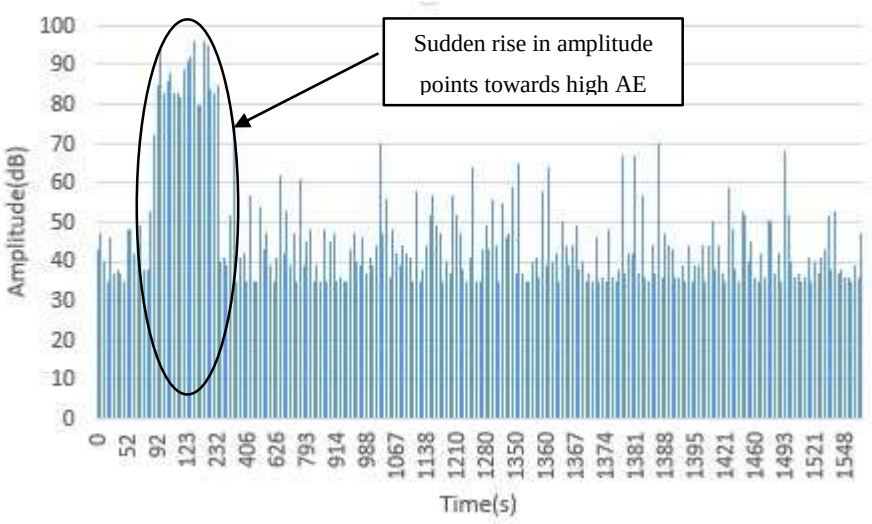


**Figure 4.2:** Amplitude vs Time graph for mild steel specimen

Figure 4.1 shows the load vs time plot obtained from UTM for the first specimen. The encircled region is where the elastic behavior mild steel shifts to plastic behavior. In the elastic region, load is directly proportional to displacement. However, after phase transitions more displacements are recorded for lesser variations in load. From the encircled region, the materials undergoes permanent deformations. Permanent deformation result in the necking region which occurs in the later stages of deformation and finally lead to the overall failure of the material. In order to relate the results with Acoustic emission data, the amplitude of AE hits Vs time is plotted as shown in Figure 4.2. It can be noted that much of the acoustic emissions were recorded before the deformation could be visually detected. After this period, load values

decreased and therefore, recorded acoustic emission were very less. However, the process of development of cracks increased. Therefore, it can be noted that AE picks up the damage much before, it reaches the surface and visually observable to naked eyes. From the Figure 4.1, it can be seen that initially, with the increase in the load during the linear elastic region of the load-displacement plot, lesser no. of AE are recorded. But after the yielding stage is reached, greater no. of AE emissions are recorded during this phase and there is decrease in the load applied. Therefore, it can be ascertained that during the initial 'linear elastic region' of load-displacement curve, no significant stress redistribution takes place which does not result in much of acoustic emission generation. However, significant stress-redistribution takes place once the yielding region is reached and therefore, most of the recorded acoustic emission are observed during this time. This is also confirmed magnitude of acoustic emission recorded as the amplitude of AE. During the initial stages, the recorded amplitudes have very less values ranging from 40-50. However, these values increase drastically during the yielding region, ranging from 45 to 100, when linear deformation are replace by plastic deformations by the magnitude of AE hits. After he yielding regions has passed, not much stress distribution takes place as most of the localization of micro voids have already taken place. And the corresponding values of acoustic emission are even far lesser than that in the yielding region (ranging from 40 to 65).

Therefore, it can be propounded that origin of plasticity in metals can be a great source of development of AE generation. This is essentially due to the localization of micro voids and the inherent defects such as like crystal dislocations, micro inclusions etc. giving rise to crack front and aiding in its progression.

**(a) Ib- Value analysis**

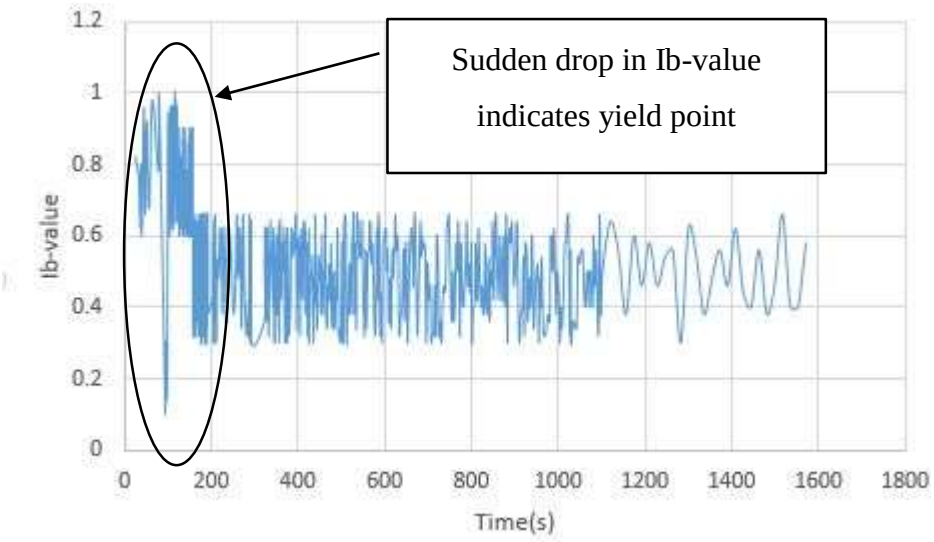


**Figure 4.3:** Ib-value vs Time graph for mild steel specimen

Ib-values analysis was also done in order to quantify the extent of damage that the material has undergone. As the material undergoes deformation, the path of travelling elastic waves which are to be recorded by AE sensors mounted on the surface of the material, gets obstructed due to the change in geometry of the material and therefore, most of AE energy gets dissipated. Therefore, the magnitude is the recorded acoustic emission is far much lesser than the actual value. Therefore, the results of AE amplitude could be misleading. In order to overcome this, Ib-value analysis was performed and it was used to bridge the strong events and the weak events.

Figure 4.3 shows the Ib-value Vs time for the material. It can be observed that the lowest Ib-values that were observed were in the range of 0.1-0.3. These values appear during the same time when the transition of the material from elastic to plastic zone is taking place. During the same time, large no. of AE are recorded with greater values of AE amplitude and, therefore, the lowest Ib-value provides the accurate indication of damage occurrence.

### 4.2.2. M3 and M4 specimens at 4 mm/min rate of loading

Two MS specimens (M-3 & M-4) were subjected to a strain rate of 4 mm/min was to ensure repeatability of acoustic emission data analysis and the results were obtained from both UTM and acoustic emission setup. The best of two plots was selected for analysis.

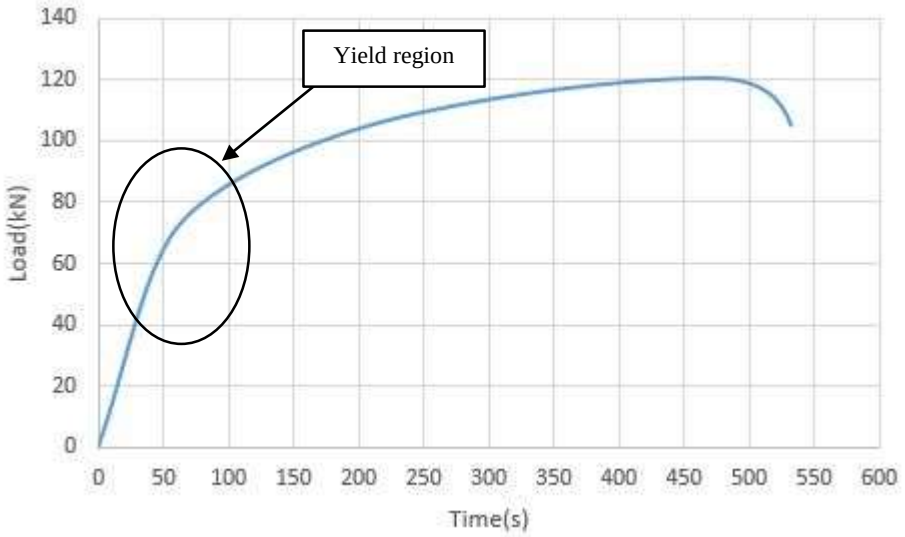


**Figure 4.4:** Load vs Time graph for mild steel specimen

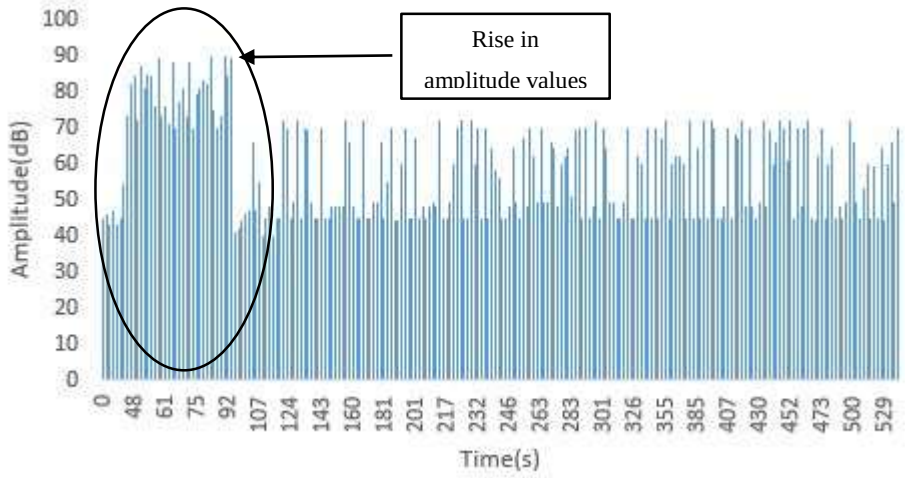


**Figure 4.5:** Amplitude vs Time graph for mild steel specimen

In this case, the yielding region occurred between 50 to 100 seconds on the load-displacement plot, marked by a circle. Due to the faster strain rates, the yielding region has occurred much earlier than in the case of 1.5 mm/min. Figure 4.5 shows the amplitude of AE hits Vs time plot for the entire duration of loading. It can be clearly observed that very less acoustic emissions are recorded in the first 50 seconds of the loading. The values of amplitudes recorded was very less ranging between 40 and 50 dB. This time interval also corresponds with the linear elastic zone of the load-displacement curve. However, from 50 to 100 seconds of loading, the rate of the AE generation increased drastically as depicted by the increased density of the amplitude plot. Also, the values of amplitude recorded during this period were very high ranging between 45 to 100 dB. This further ensures that most of the deformations took place during this period only.

**a) Ib-value analysis**

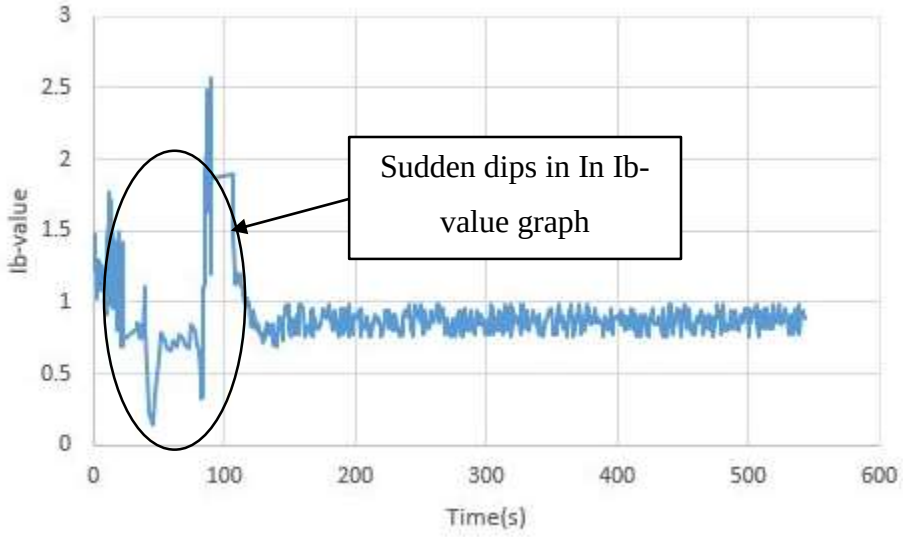


**Figure 4.6:** Ib-value vs Time graph for mild steel specimen

Ib-values analysis was also performed to quantify the damage and to validate the acoustic emission results in contrast with load-displacement curves as shown in figure 4.6 Few dips are reported in graph during the same time ranging from 50 to 100 seconds, indicating that most of the damage that occurred during this period itself. The lowest Ib-values that were observed was ranging between 0.2 and 0.5. The results from Ib-value analysis is in total coherence from the findings of Load-displacement curve and amplitude of AE hits.

### 4.2.3. M5 and M6 specimens at 8 mm/min rate of loading

Two MS specimens (M-3 & M-4) were subjected to a strain rate of 8 mm/min was to ensure repeatability of acoustic emission data analysis and the results were obtained from both UTM and acoustic emission setup. The best of two plots was selected for analysis.

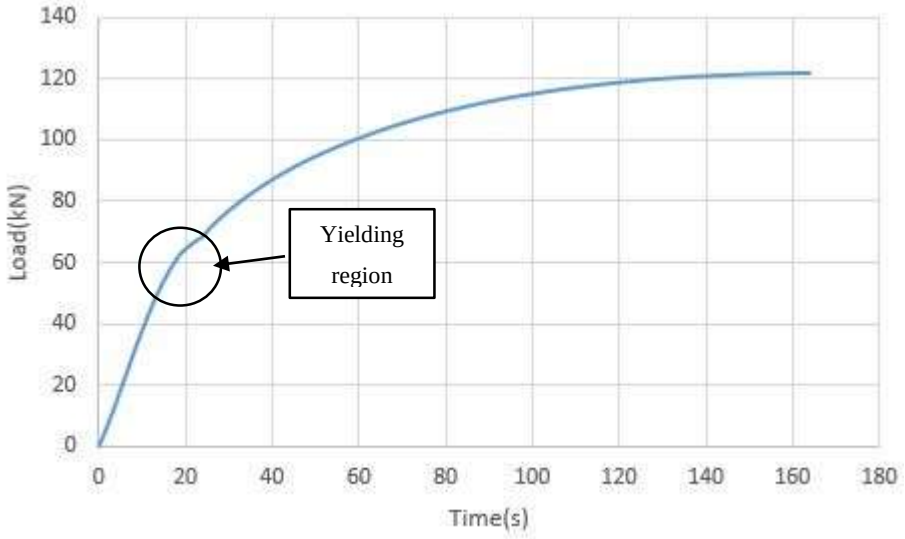


**Figure 4.7:** Load vs Time graph for mild steel specimen

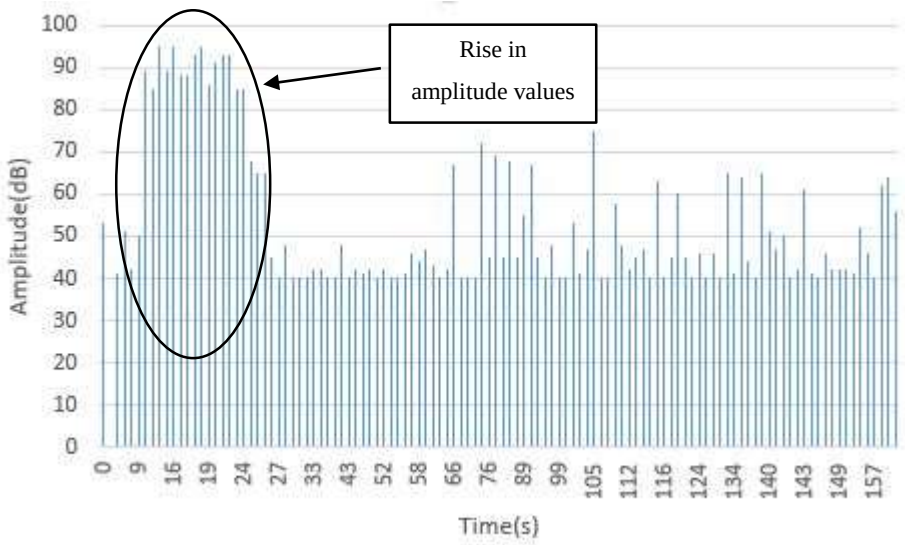


**Figure 4.8:** Amplitude vs Time graph for mild steel specimen

The strain rate was then increased to 8 mm/min to observe the variation of Ib value with increased loading rates. The yielding region was observed from 18 to 30 seconds of load application. Figure 4.8 showed the amplitude Vs time plot for the entire duration of the experiment. The graph indicates that there was very less acoustic emissions recorded initially for few seconds of loading but it increased drastically after first 18 seconds and acoustic emission generation increased upto 30 seconds of loading. The values of amplitude that were recorded were also very high ranging between 45 to 100 dB. This further confirms that most of stress redistribution took place during this very period. The Ib-value analysis plot also suggested that

during this period ranging from 18 to 30 seconds, most of the damage has occurred. The lowest Ib-values below 0.2 were also recorded during this period.

**a) Ib-value analysis**

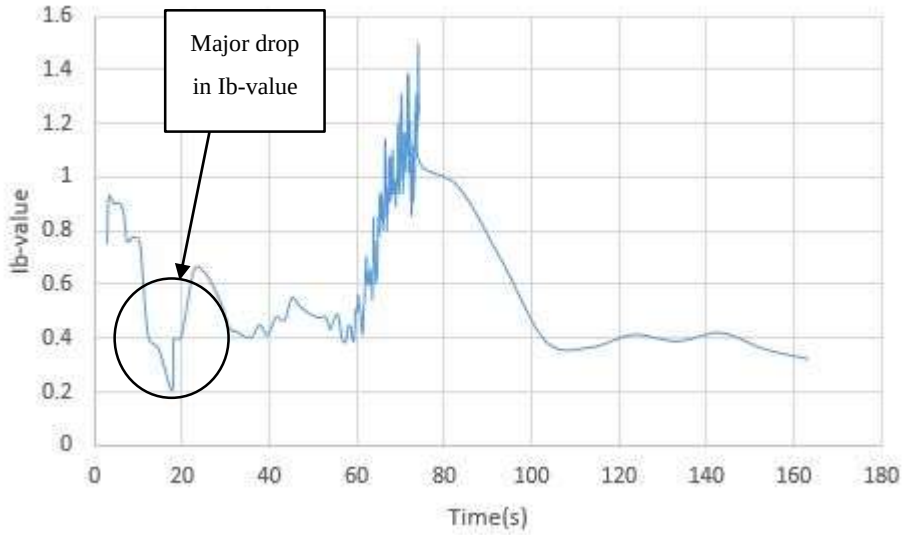


**Figure 4.9:** Ib-value vs Time graph for mild steel specimen

From the Ib-value analysis (figure 4.9) of samples subjected to three different strain loadings, it can be clearly observed that no. of dips recorded during the yielding region (where maximum stress changes took place) decreased with the increase in loading. The samples that was subjected to strain loading of 8mm/min resulted in only one dip. Therefore, it can be inferred that AET has the capacity to pick up damages at all kinds of loadings at different rates but it gives a much better idea when it is subjected to slower rate of loadings. The lower Ib value was found approximately 0.2 for 8mm/min. in terms of appearance, the lower Ib value appeared prior to lower Ib values in 1.5mm/min and 4mm/min.

## 4.3. Results from brittle materials

In order to investigate the efficacy of acoustic emission to quantify damage in brittle materials, Concrete and FRP was tested using acoustic emission. Both the concrete and FRP was subjected to three different rates of loading as was in case of mild steel. The concrete was tested in compression and FRP was tested in tension. The results of concrete cubes for different loading rates are as:

### 4.3.1. C1 and C2 specimens at 0.5mm/min of loading rate

Two concrete cubes were tested in compression at 0.5 mm/min rate of loading and acoustic emissions (AE) were also recorded.

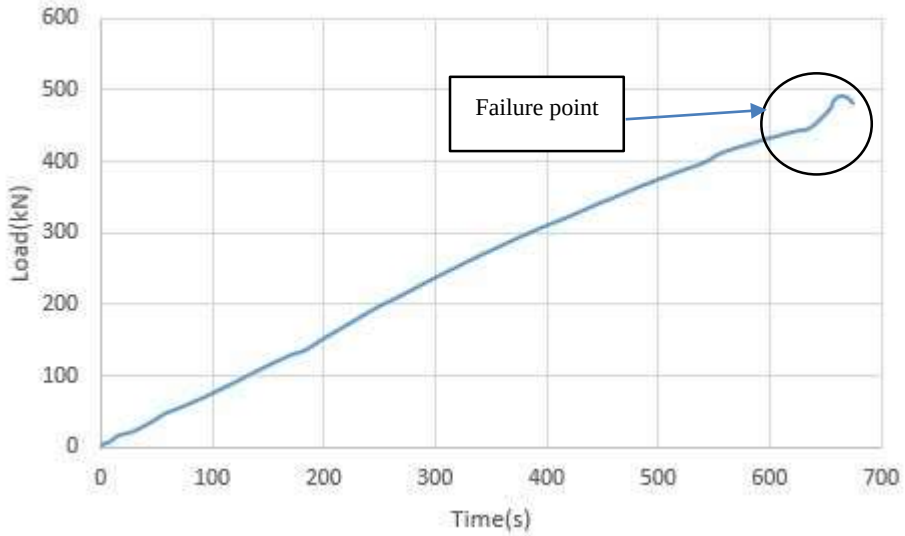


**Figure 4.10:** Load vs Time for concrete specimen

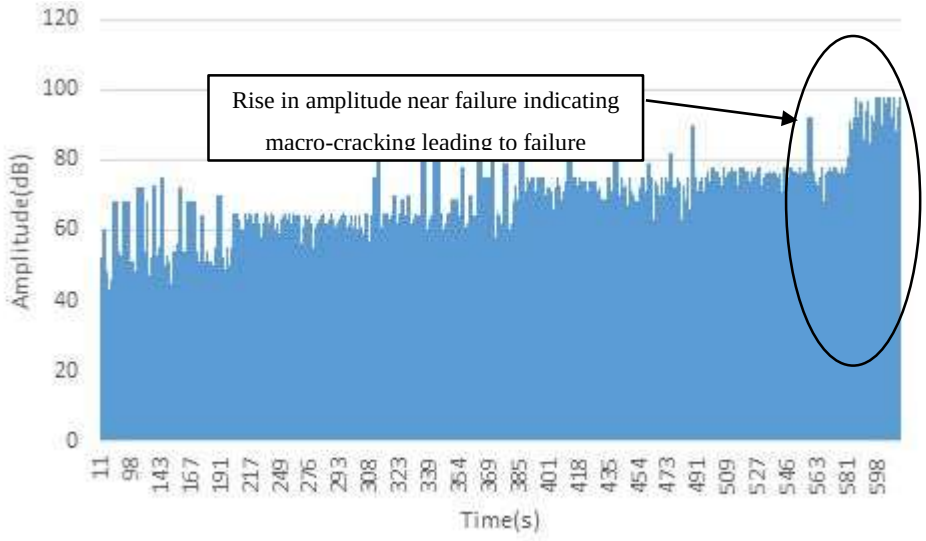


**Figure 4.11:** Amplitude vs Time for concrete specimen

The yielding region of concrete was found to be ranging from 580 to 650 seconds after which it failed in compression. The amplitude of acoustic emissions was also plotted against time. It is observed that the values of amplitude recorded were from 40 to 55 dB in the initial stages of loading. However, as the loading increased, the values of recorded amplitudes also increased in such a way that at the point of yielding and thus failure, the values of amplitude were ranging

from 40 to 100 dB. Therefore, initial lower values of amplitude signified the development of micro-cracks in concrete. With the increase in loading, the width of micro-cracks increased greatly (the values of amplitude increasing upto 75 dB) and finally micro-cracks taking the shape of macro-cracks and therefore ultimately leading into failure.

**a) Ib-value analysis:**

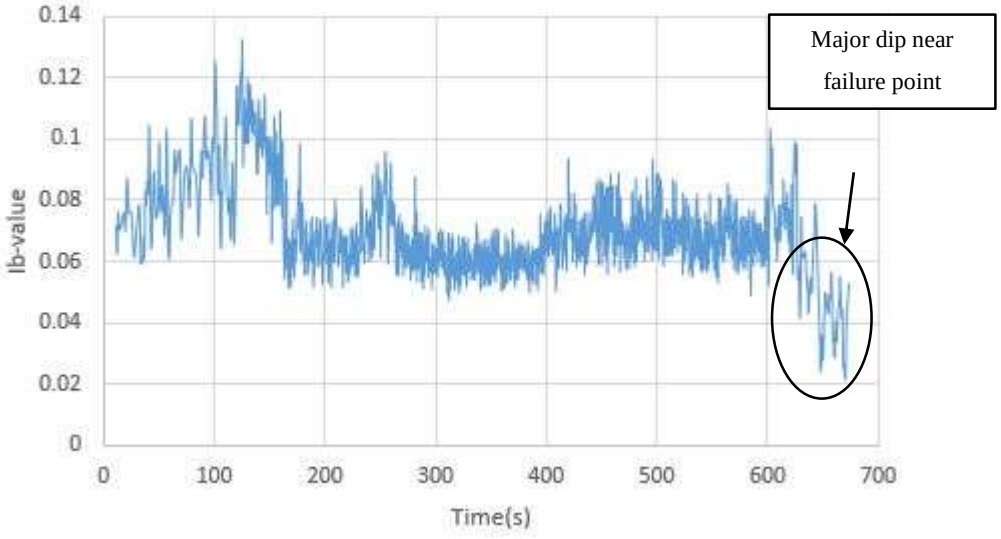


**Figure 4.12:** Ib-value vs Time graph for concrete specimen

Since concrete is a heterogeneous material and loading results in the development of micro-cracks initially, therefore, there is a greater possibility that large number of acoustic emission that were to be recorded by AE sensors may either get lapsed due to higher attenuation or received with lower signal amplitudes. Therefore, in case of concrete, the results could be highly misleading. For this purpose, we have also performed Ib-value analysis. Figure 4.12 shows the Ib-value curve with time for the entire duration of loading. IT can be clearly seen that the Ib-value starts decreasing immediately after few seconds of loading and afterwards, it goes on decreasing so much so that the entire Ib-value plot remains below the 0.1 value. The lowest Ib-values were observed during the yielding region itself.

### 4.3.2. C3 and C4 specimens at 1.0mm/min of loading rate

Two concrete cubes were tested in compression at 1.0 mm/min rate of loading and acoustic emissions were recorded simultaneously.

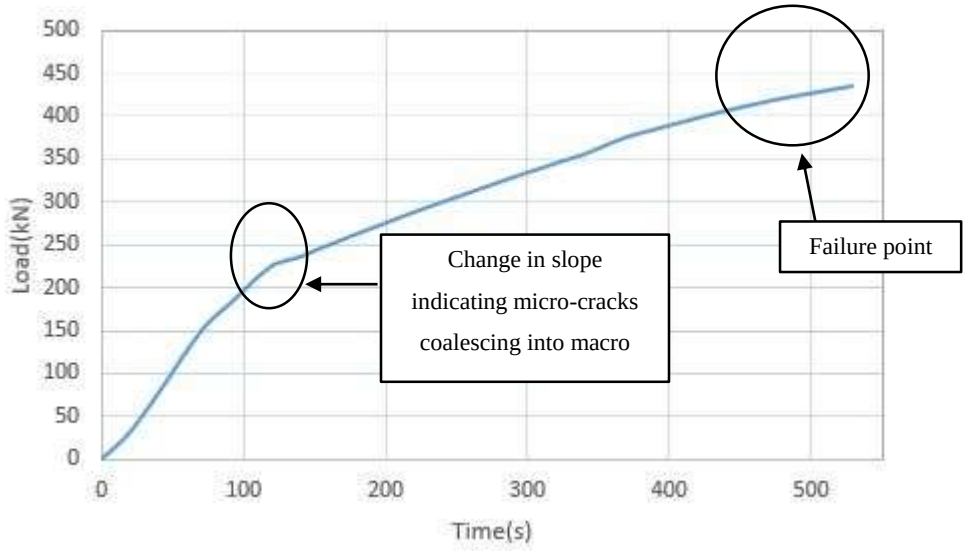


**Figure 4.13:** Load vs Time graph for concrete specimen

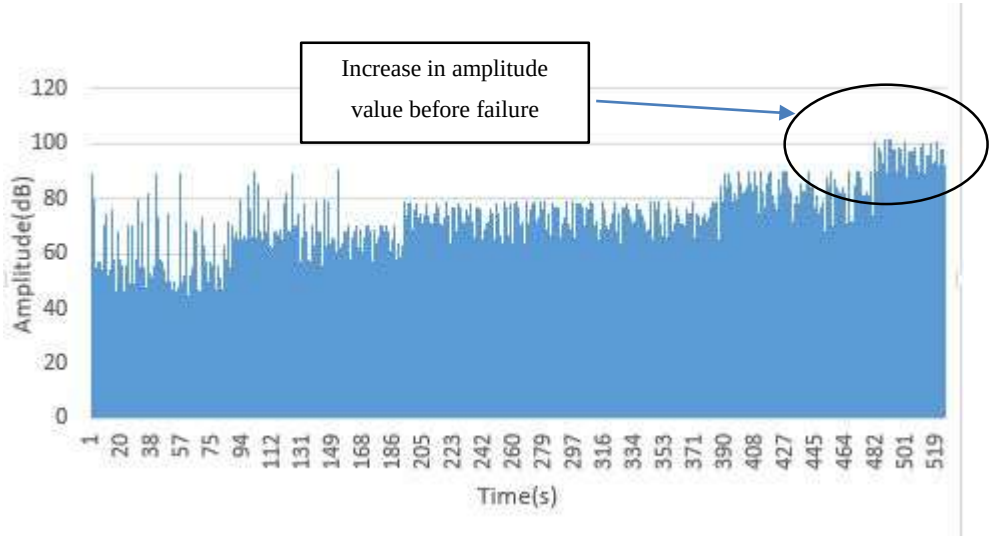


**Figure 4.14:** Amplitude vs Time graph for concrete specimen

From the load-time graph (figure 4.13), it can be observed that time of failure reduced than the previous sample tested at 0.5 mm/min. AE amplitudes were also plotted against time for the entire duration of loading. Similar behavior was observed with acoustic emissions of smaller amplitudes ranging from 40 to 55 dB recorded during the initial loading. This gradually increased and the values ranging upto 100 dB were recorded as the specimen reached failure.

**(a) Ib-value analysis:**

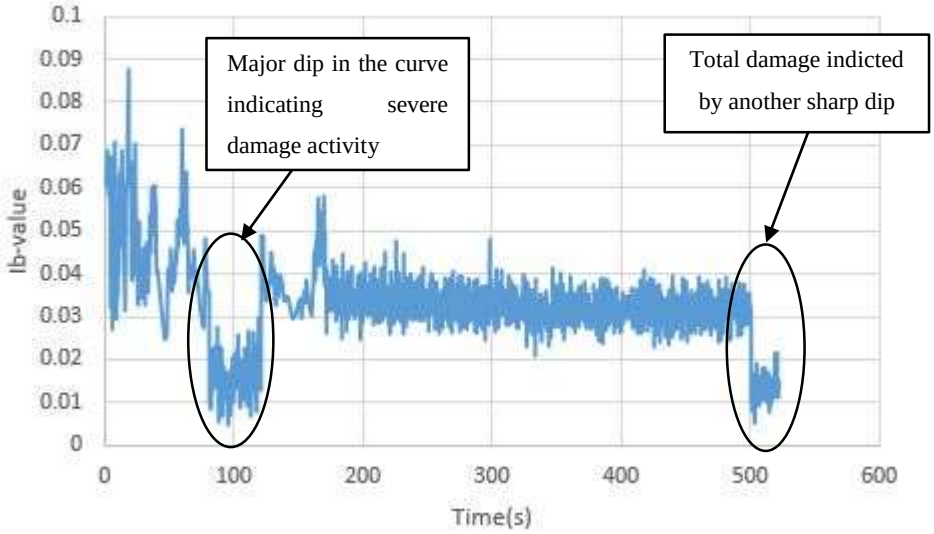


**Figure 4.15:** Ib-value vs Time graph for concrete specimen

Figure 4.15 shows the Ib-value plot Vs time. It can be clearly seen that dips are observed throughout the length of the duration of loading. And the lowest Ib-values are observed near the failure of the Specimen. This is very much in coherence with the AE amplitudes and and the load-time plot.

### 4.3.3. C5 and C6 specimens at 1.5mm/min of loading rate

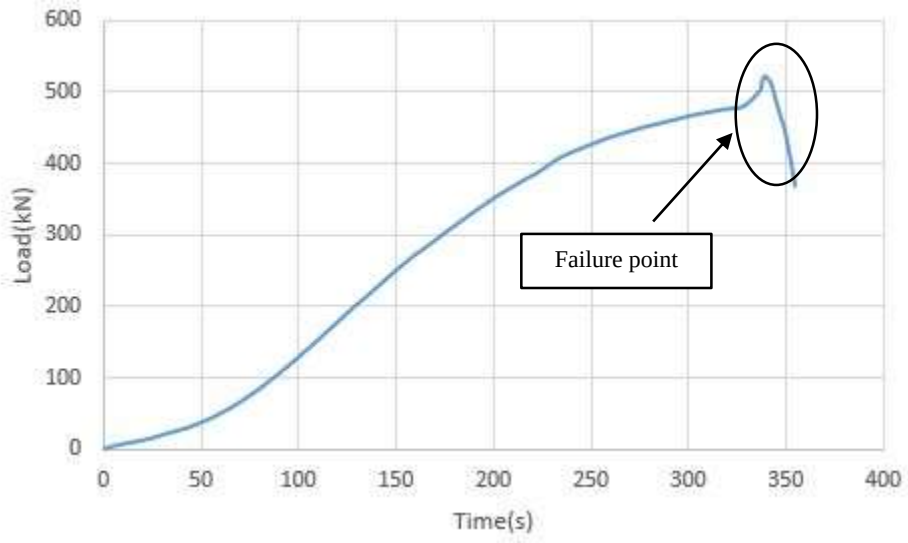


**Figure 4.16:** Load vs Time graph for concrete specimen

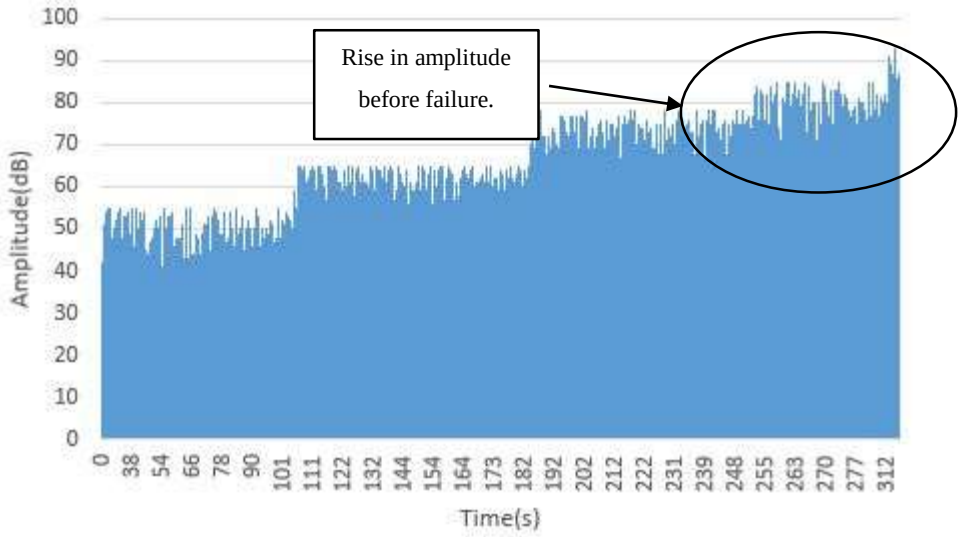


**Figure 4.17:** Amplitude vs Time graph for concrete specimen

Two concrete cubes were tested under compression and load vs time curve was plotted as shown in the figure 4.16. Acoustic emission were also recorded for the entire loading time. The failure for this specimen occurred much earlier than the previous two specimens. Amplitude of AE hits vs time was also plotted as shown in Figure 4.17 can be ascertained that a very similar behaviors was observed for the concrete specimen wherein lesser values of amplitude were recorded during the initial stages of loading and it further increased as the loading increased with time.

**(a) Ib-Value analysis:**

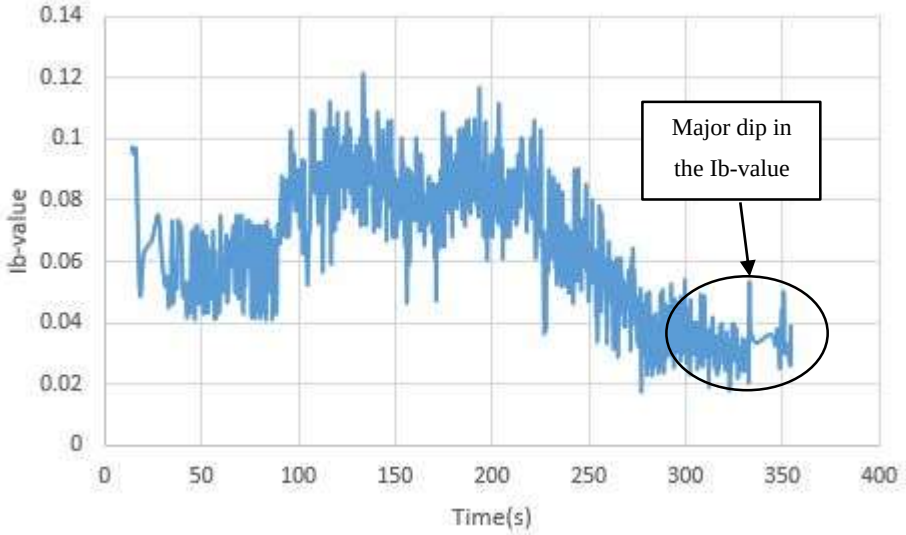


**Figure 4.18:** Ib-value vs Time graph for concrete specimen

The plot of Ib-value analysis vs time is shown in Figure 4.18. It can be clearly seen that significant no. of dips are recorded during the entire loading time. And the Ib-value that are observed are very low. This further points towards the fact that Ib-value analysis provides the damage indication throughout the loading and therefore, the deformation of the specimen.

## 4.4. Results from composite materials

Two types of composite specimens were used 1) Glass fiber reinforced polymer 2) Carbon fiber reinforced polymer with carbon nanotubes. The specimens were prepared in the lab. The specimens were tested in tension and acoustic emission were also recorded for the entire loading time.

### 4.4.1. GF1 and GF2 at 0.25mm/min of loading rate

Two specimens of GFRP were tested in UTM under tension and the best was selected for analysis. Figure 4.19 shows the load-time curve of the composite specimen tested at 0. 25 mm/min of loading rate.

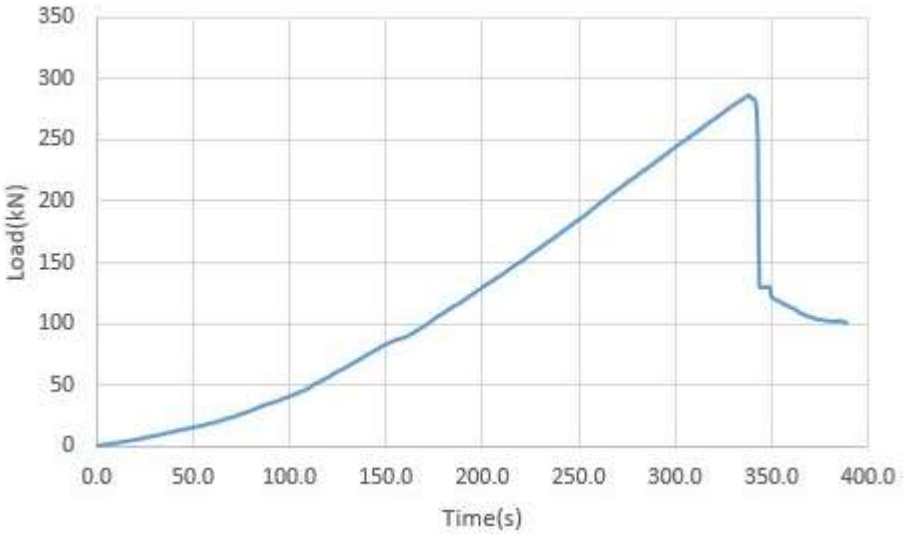


**Figure 4.19:** Load vs Time graph for GFRP specimen

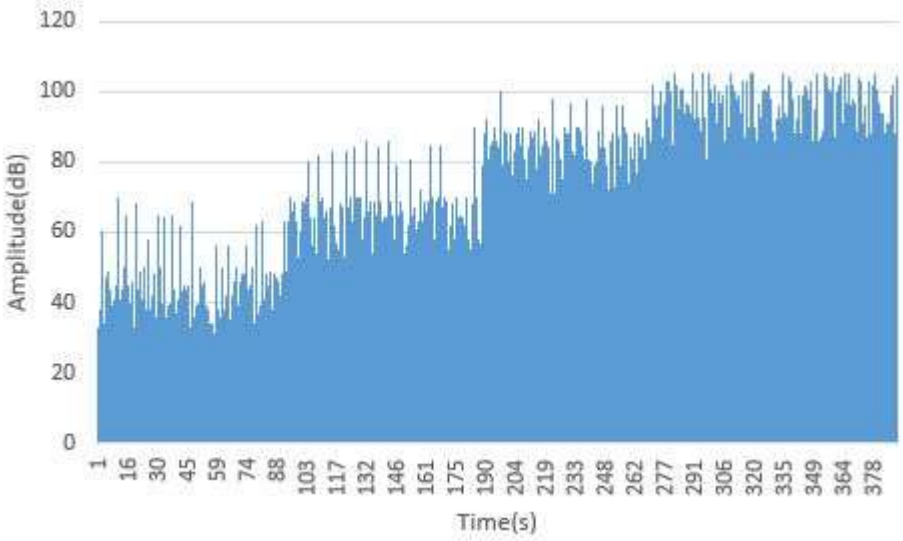


**Figure 4.20:** Amplitude vs Time graph for GFRP specimen

The yielding/failure occurred after 350 seconds of loading. Figure 4.20 shows the amplitude vs time of the recorded AE hits. The values of amplitude exhibited a distinctive step type variation. The values increased from 40 dB and ranged upto 100 dB until the end of the experiment. This kind of variation signifies the progressive damage as the increasing values of amplitude in step wise indicates that increase in loading results in increasing values of amplitude.

**(a) Ib-Value analysis:**

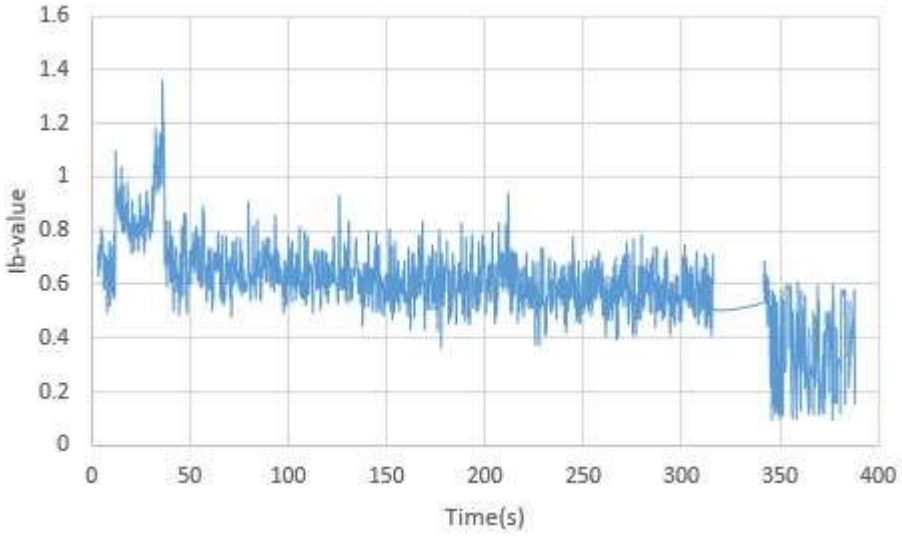


**Figure 4.21:** Ib-value vs Time graph for GFRP specimen

Figure 4.21 shows the Ib-value plot against time for the entire duration of the loading. From the graph it can be clearly seen that significant no of dips are recorded. The lowest Ib-values were

observed when the specimen reached the failure point. Moreover, the Ib-value are observed to range between 0.02 to 0.06 which is very less and hence signifies progressive damage that the GFRP undergoes.

### 4.4.2. GF3 and GF4 at 0.5mm/min of loading rate

Two specimens of GFRP were tested under tension and best was selected for analysis. Figure 4.22 shows the Load-time plot of the GFRP for entire loading duration.

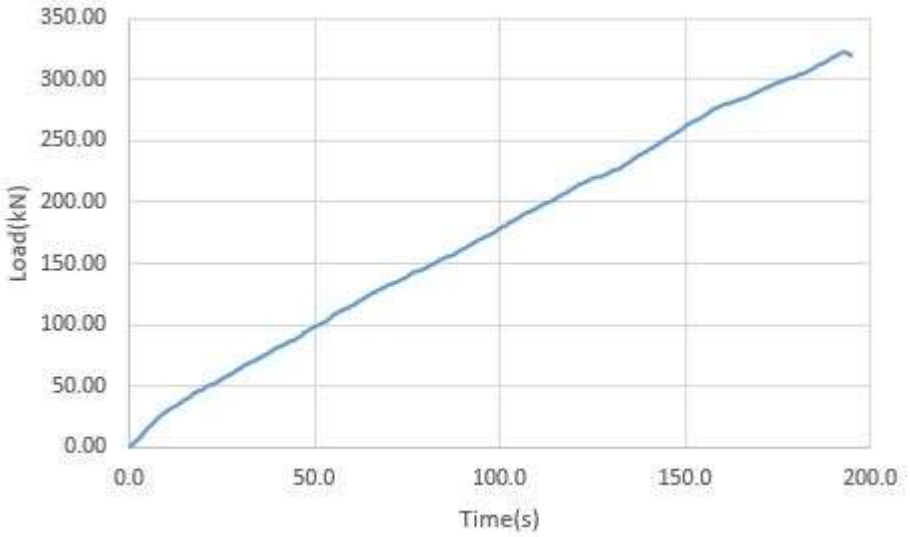


**Figure 4.22:** Load vs Time graph for GFRP specimen

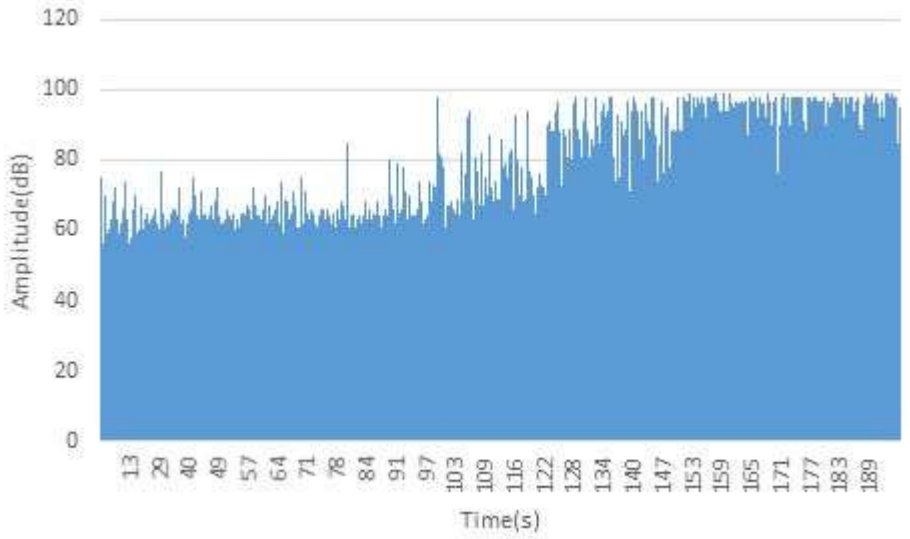


**Figure 4.23:** Amplitude vs Time graph for GFRP specimen

The failure in this case has occurred around 190 seconds of loading which is much lesser than the previous case. The plot of amplitude Vs time is shown in the Figure 4.23, it is clearly visible from the plot that though the damage was progressive but it experienced lesser steps than the one

was tested at a slower rate. Initially, the lower values of amplitude were recorded and it increased gradually with load and by the time failure point was reached, the recorded value of amplitude was highest. We can ascertain the failure was relatively abrupt than it was in the previous case.

**(a) Ib-value analysis:**

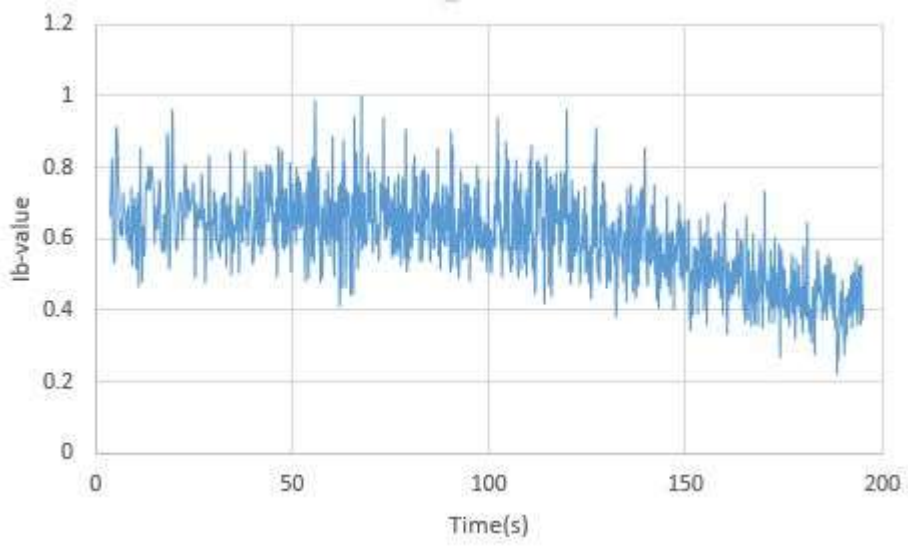


**Figure 4.24:** Ib-value vs Time graph for GFRP specimen

Figure 4.24 shows the plot of Ib-value analysis for the GFRP specimen loaded under tension. Very low Ib-values were recorded for the entire duration of the loading. Significant no. of dips are recorded for the entire duration of the experiment. Therefore, it can be inferred that damage starts from the initiation of the experiment and it goes upto severe indicated by low Ib-values before the failure.

### 4.4.3. GF5 and GF6 at 1.0mm/min of loading rate

Two specimens of GFRP were tested under tension at the rate of 1 mm/min and best one was selected for analysis. Acoustic emissions were also recorded for the entire loading time.

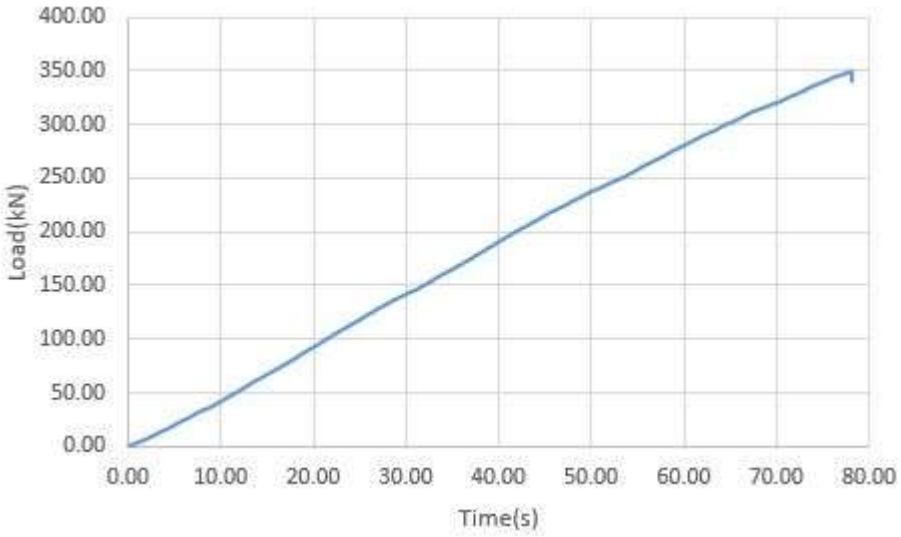


**Figure 4.25:** Load vs Time graph for GFRP specimen

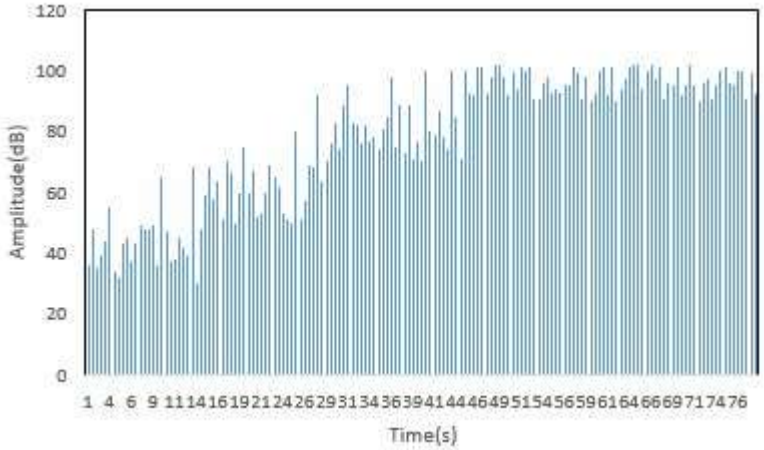


**Figure 4.26:** Amplitude vs Time graph for GFRP specimen

Figure 4.25 shows the load-time plot for the specimen and it can be seen that yielding region occurs at 70-80 seconds of applied load. The plot of amplitude of AE hits versus time indicated that lower values of amplitude were recorded initially and afterwards, there is sudden increase in the values of amplitude indicating a brittle failure.

**(a) Ib-value analysis:**

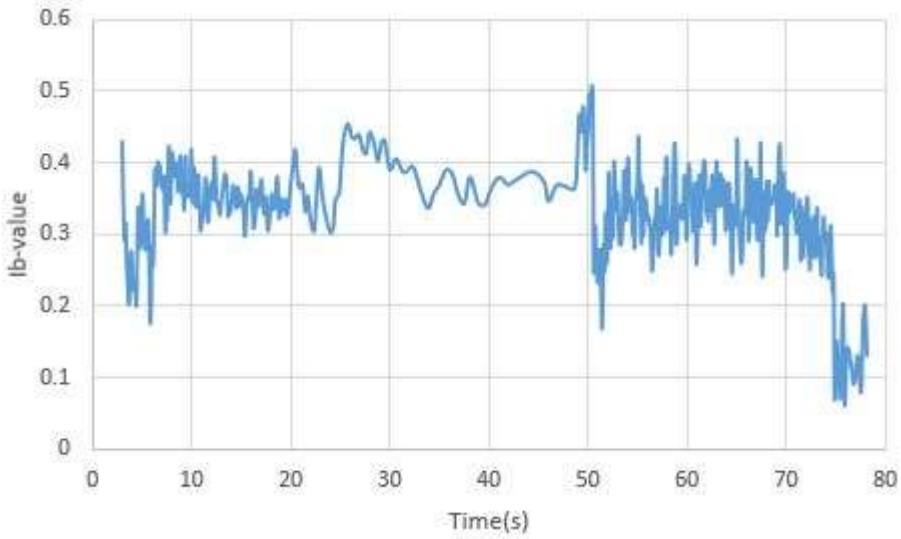


**Figure 4.27:** Ib-value vs Time graph for GFRP specimen

Figure 4.27 shows the plot of Ib-value Vs time for entire duration of the load application. It can be clearly seen that very low Ib-values are recorded for most of the duration of the experiment. However, in the graph, it is clearly visible that after half of the time of load application, there is sudden drop in the Ib-value which continued to drop further. This also indicates the occurrence of sudden damage as was indicated by the AE amplitude.

### 4.4.4. GF7 and GF8 at 1.5mm/min of loading rate

Two specimens of GFRP were tested under tension and best was selected for analysis. The load-time plot is shown in the Figure 4.28.

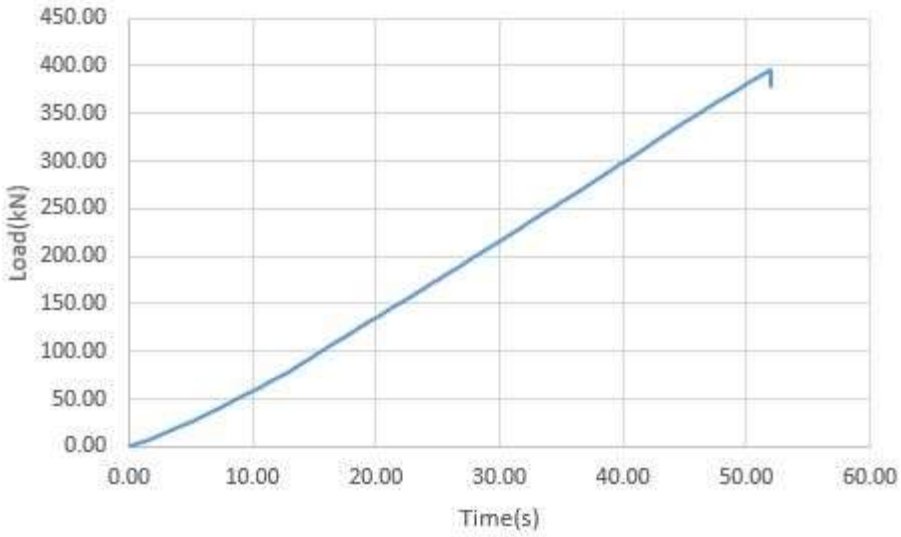


**Figure 4.28:** Load vs Time graph for GFRP specimen

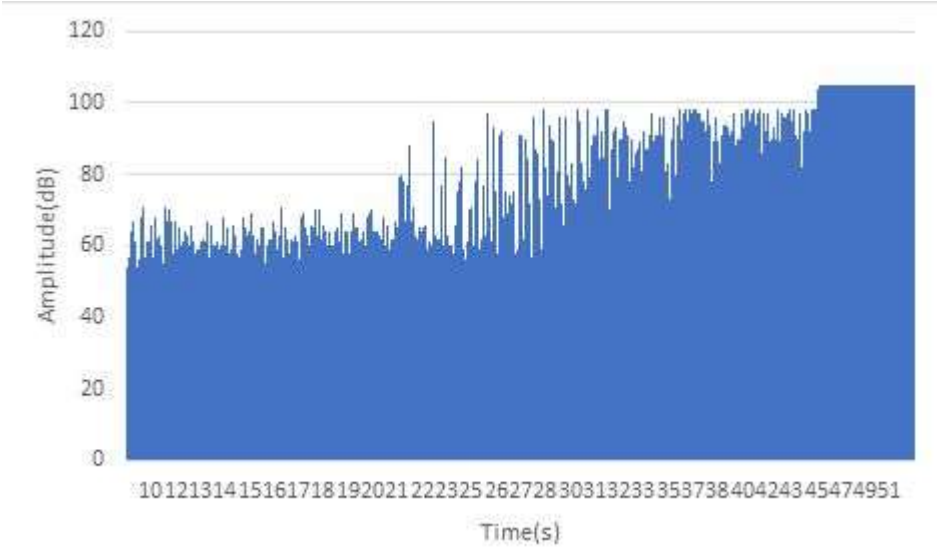


**Figure 4.29:** Amplitude vs Time graph for GFRP specimen

It can be clearly observed that the yielding/failure occurred only after 55 seconds of loading. Figure 4.29 shows the amplitude of acoustic emission versus time plot wherein it can be easily ascertained that the there was no transition stage of damage and it occurred suddenly. The values of amplitude of acoustic emission increased from 45 to 100 dB in a very short period of time. This further indicates a brittle failure.

**(a) Ib-Value analysis:**

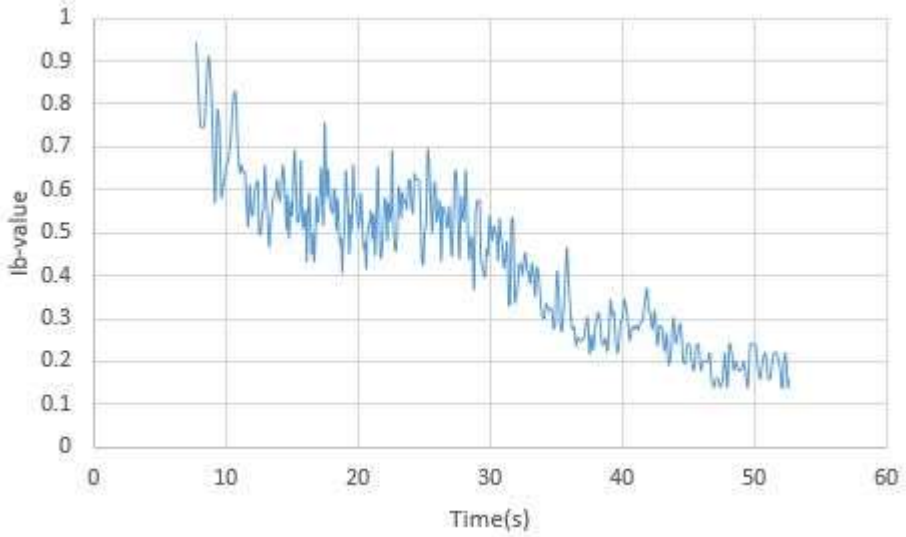


**Figure 4.30:** Ib-value vs time graph for GFRP specimen

From the Ib-value analysis plot shown in figure 4.30, it can be clearly seen that after an initial loading, there is a consistent and sudden fall in the Ib value plot indicating faster damage and therefore brittle failure.

### 4.4.5. GF9 and GF10 at 2.0mm/min of loading rate

Two specimens of GFRP were tested under tension and best was selected for analysis. The load-time plot is shown in the figure 4.31.

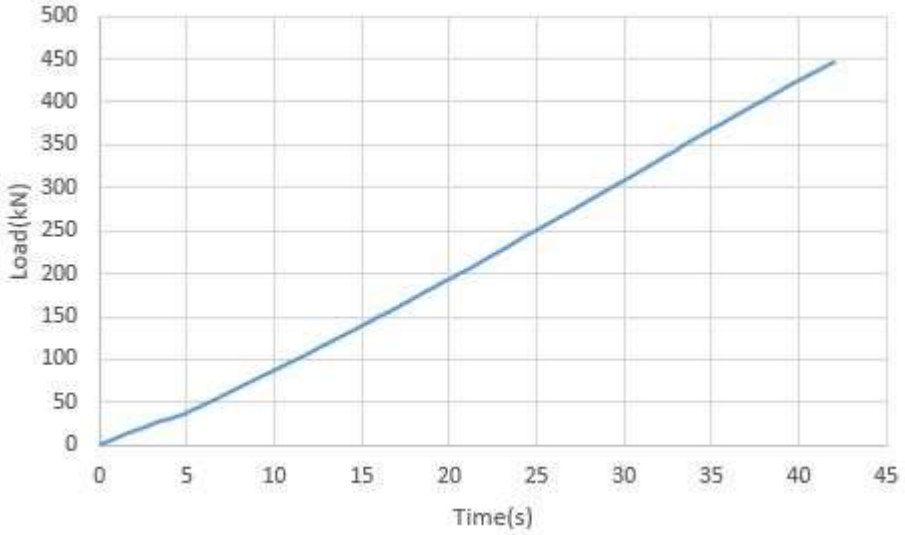


**Figure 4.31:** Load vs Time graph for 5th GFRP specimen

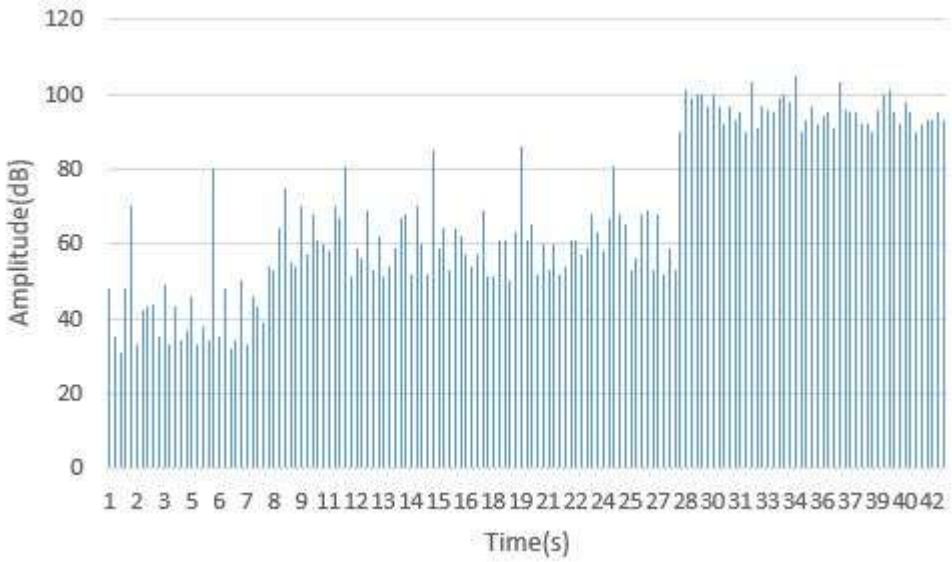


**Figure 4.32:** Amplitude vs Time graph for GFRP specimen

It can be clearly observed that the yielding/failure occurred only after 5 seconds of loading. The plot of AE amplitude versus time very well indicates a quick and sudden failure of the specimen where lower amplitudes were recorded in the initial stages of loading and when the specimen was reaching failure, the amplitude values increased suddenly indicating a brittle failure.

**(a) Ib-value analysis:**

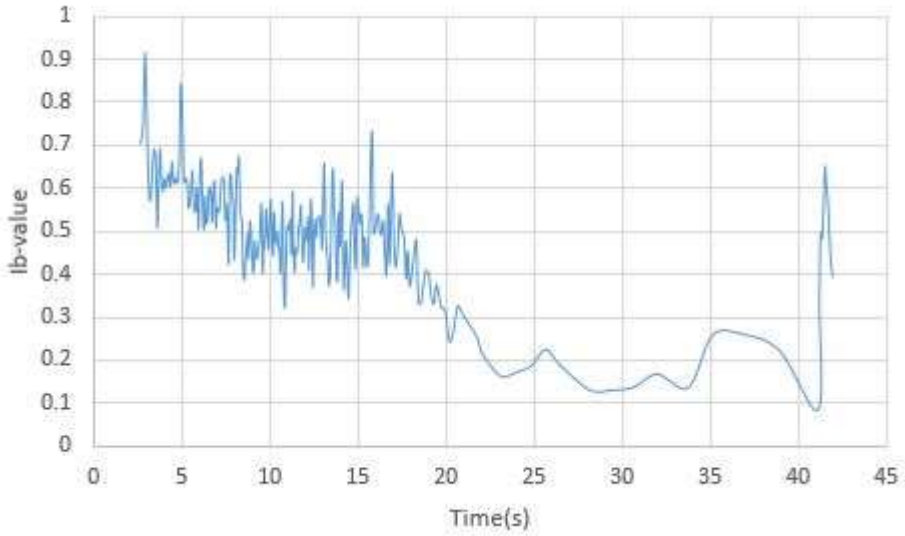


**Figure 4.33:** Ib-value vs Time graph for GFRP specimen

From the Ib-value analysis plot (figure 4.33), it can be clearly seen that the Ib-value fell drastically after initial stages of loading indicating severe damage.

The lower Ib value was found 0.9 at 2mm/min of loading rate. Due to less time taken by the specimen, at the end of testing Ib value is fluctuating less because cracks were growing at high speed. And lower value of Ib was found prior then 0.25mm/min, 0.5mm/min, 1mm/min, 1.5mm/min.

Second type of composite in which carbon fiber was used and CNT nanofiller was added to the material. Tensile testing at different loading rates was done and acoustic emissions were recorded for the entire duration of the loading for all the specimens.

### 4.4.6. CF1 and CF2 at 0.5mm/min of loading rate

Two specimens of CFRP were tested under tension and best was selected for analysis. The load-time plot is shown in the figure 4.34.

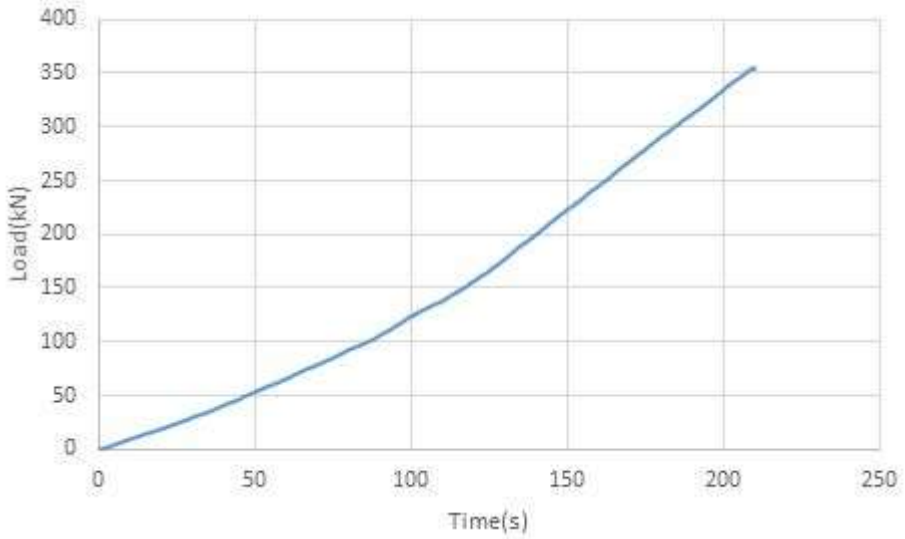


**Figure 4.34:** Load vs Time graph for CFRP specimen

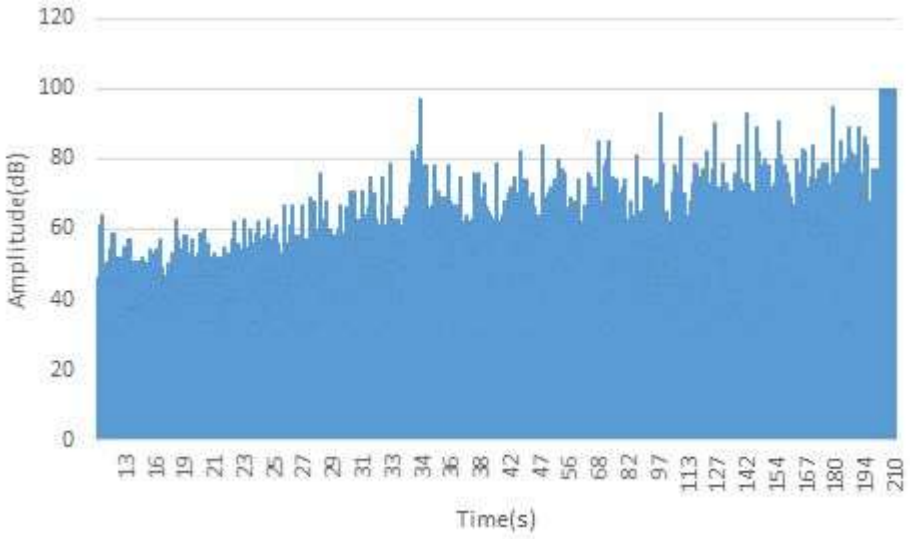


**Figure 4.35:** Amplitude vs Time graph for CFRP specimen

It can be clearly observed that the yielding/failure occurred only after 210 seconds of loading. The plot of AE amplitude versus time shown in the Figure 4.35 clearly indicates that damage was progressive and gradual. The value of AE amplitude increased with loading rate.

**(a) Ib-Value Analysis:**

The plot of Ib-value versus time of loading is shown in the figure 4.36.

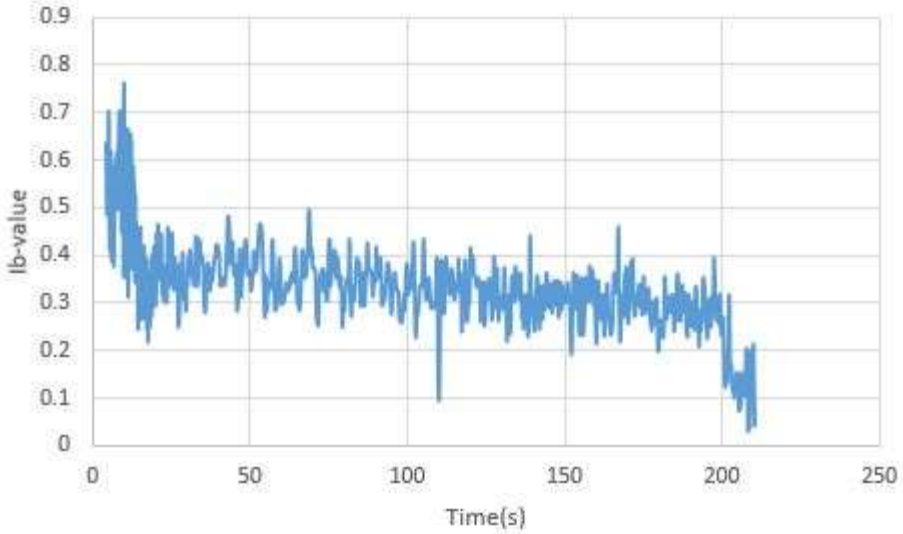


**Figure 4.36:** Ib-value vs Time graph for CFRP specimen

Various significant dips were observed during the entire duration of loading. However, the depth of dips kept on increasing indicating that the severity of the damage increased with loading rate.

### 4.4.7. CF3 and CF4 at 1.0mm/min of loading rate

Two specimens of GFRP were tested under tension and best was selected for analysis. The load-time plot is shown in the figure 4.37.

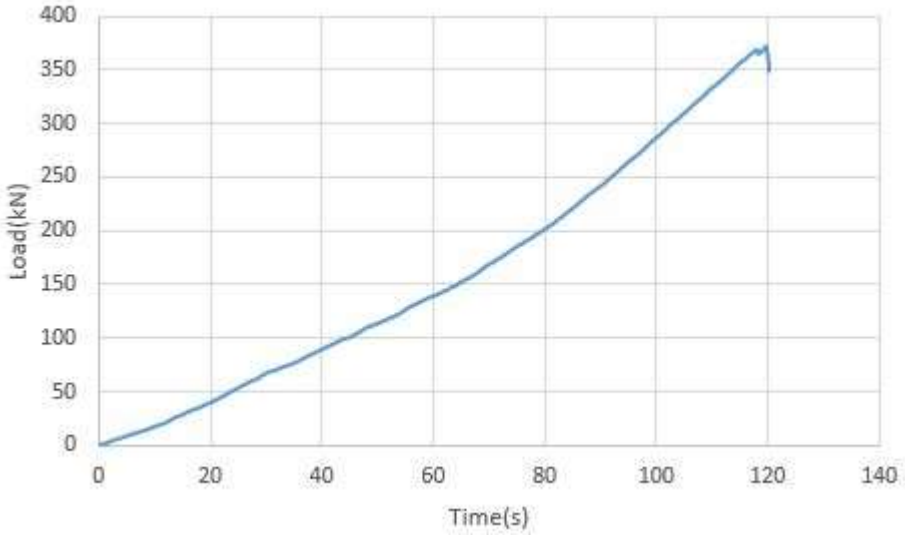


**Figure 4.37:** Load vs Time graph for CFRP specimen

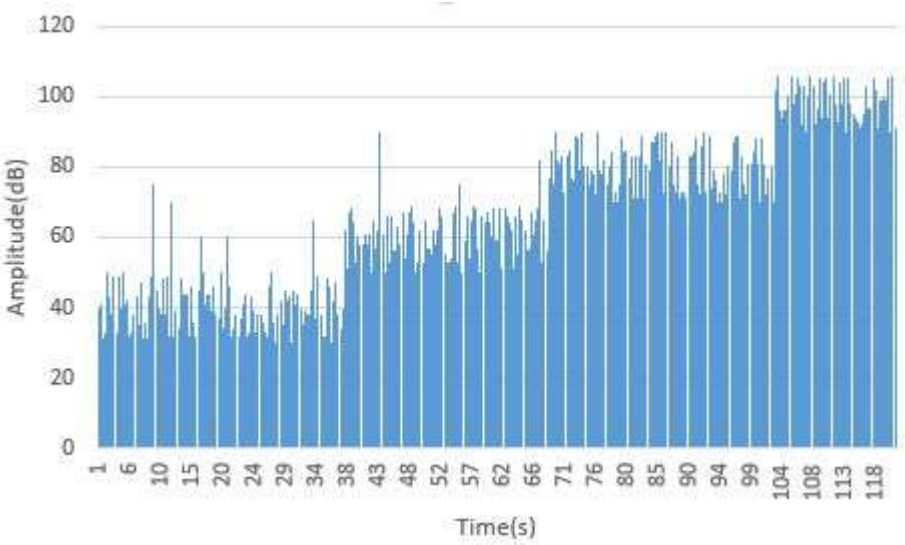


**Figure 4.38:** Amplitude vs Time graph for CFRP specimen

It can be clearly observed that the yielding/failure occurred only after 120 seconds of loading. From the amplitude Vs time plot of AE, it can be clearly seen that the damage progression was gradual as in the values of AE amplitudes increased gradually with rate of loading. However, in the later stages when the specimen was about to reach failure, there is sudden increase in the values of recorded AE amplitudes slightly indicating a brittle failure.

**(a) Ib-value analysis:**

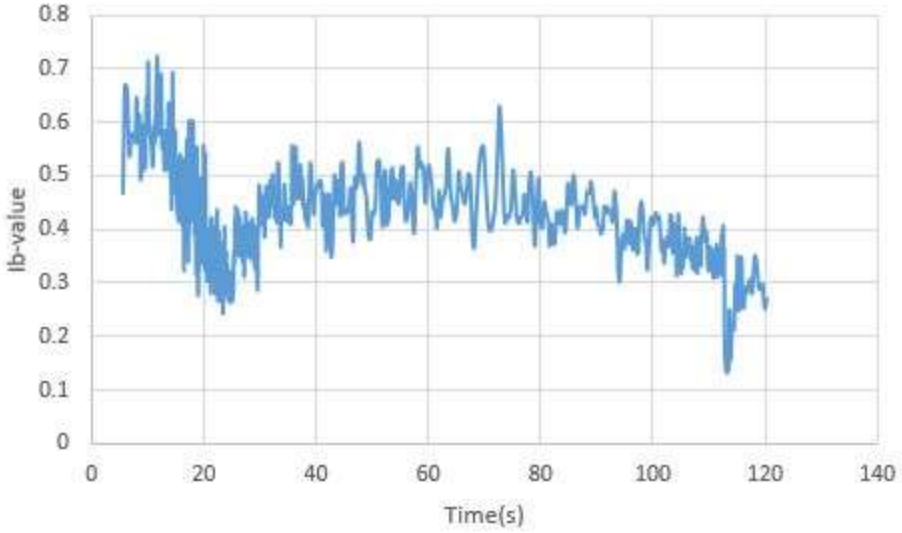


**Figure 4.39:** Ib-value vs Time graph for CFRP specimen

The Ib-value vs time is shown in the figure 4.39 for the entire duration of the loading and it can be clearly seen that there is an initial dip in the curve and afterwards, it remained constant for the entire duration. However, in the later stages, another sharp dip was observed indicating final failure. Ib-value, therefore, indicates the damage progression throughout the loading time.

### 4.4.8. CF5 and CF6 at 2.0mm/min of loading rate

Two specimens of GFRP were tested under tension and best was selected for analysis. The load-time plot is shown in the figure 4.40.

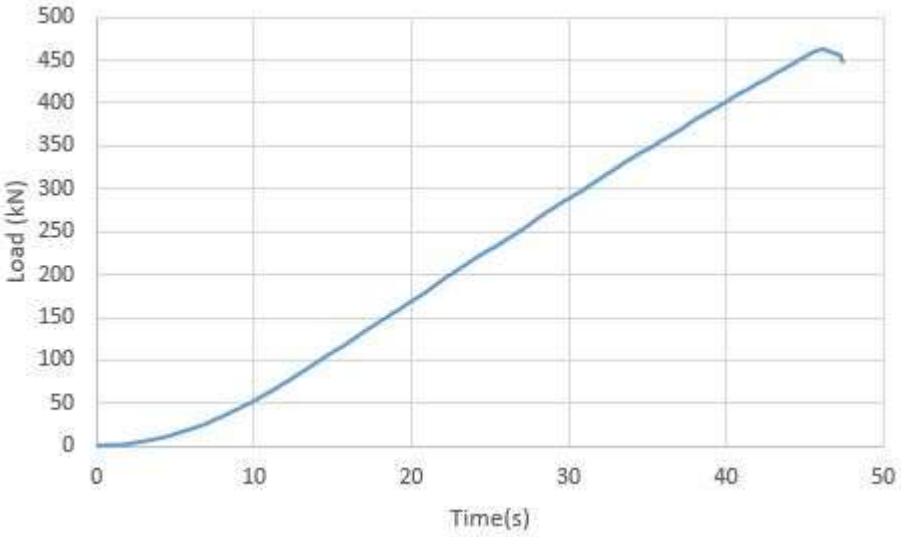


**Figure 4.40:** Load vs Time graph for CFRP specimen

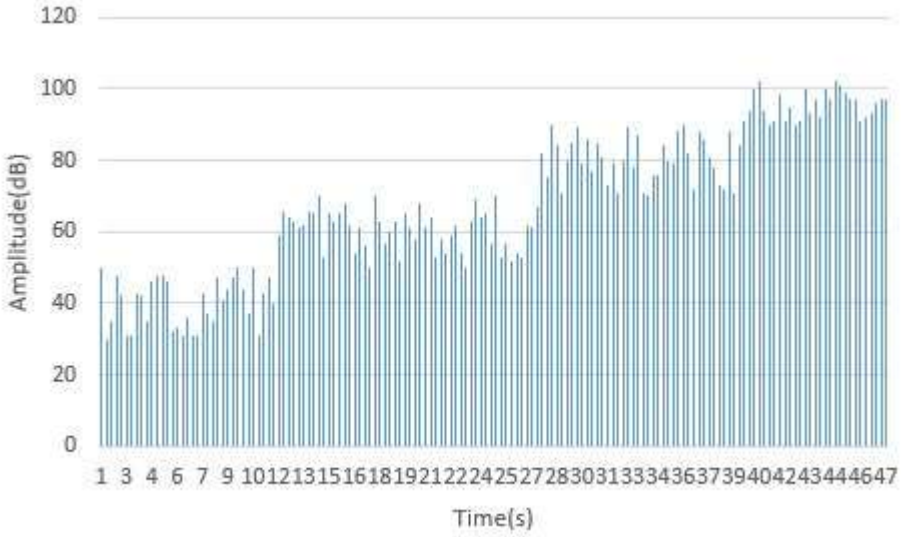


**Figure 4.41:** Amplitude vs Time graph for CFRP specimen

It can be clearly observed that the yielding/failure occurred only after 45 seconds of loading. From the amplitude-time graph (figure 4.41), it can be clearly seen that failure is abrupt and brittle in nature. The values of AE amplitude suddenly increase to maximum i.e. upto 100 dB from 45 dB.

**a) Ib Value analysis:**

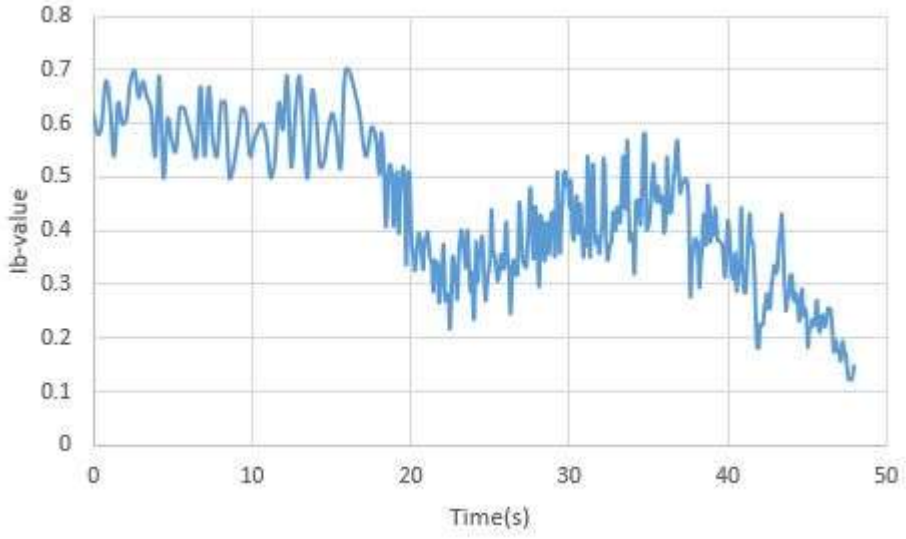


**Figure 4.42:** Ib-value vs Time graph for CFRP specimen

From the Ib-value plot, it can be clearly ascertained that there is a sudden fall in the curve after half of loading was done. This indicates that severe damage start to occur after 25 second itself while the specimen failed after the 40 seconds.

Therefore, it can be concluded that acoustic emission gives better results only when the FRP specimen were loaded at slower rates where in the damage progression was gradual in comparison to the case where the damage was abrupt, at higher loading rates. However, AE proves to effective in almost all the cases of loading rates.

## 4.5. Effectiveness of Ib-value analysis for different materials

In this study, Ib-value analysis was successfully performed on a variety of materials such as mild steel, concrete and FRP composites. It was observed that Ib-value significantly distinguished the damage patterns as per the materials. In case of the mild steel specimens, Ib-value exhibited a significant dip in the curve at the same time when yielding occurred and for the remaining duration, it remained somewhat constant. This further implies that Ib-value successfully detected the dynamic region of damage in mild steel which is yielding region during which maximum no. of AE hits are recorded. Ib- value analysis gives better results at lower loading rates indicating Acoustic emission technique gives better results at slow loads.

In case of the concrete specimens, Ib-value plot dropped consistently throughout the loading time. This further indicates that damage in concrete is progressive unlike mild steel specimens.

However, two major drops were observed for 0.5 mm/min loading rate, indicating the completion of micro cracking and major cracking. The second drop was at the same time of the failure indicating sudden failure after the major damage was induced. Whereas in other loading rates, the only one major drop was observed during i.e., near the failure time of the specimen. This further indicates that AE performs much better at lower loading rates.

In case of the composite materials, Ib-value tends to increase at the beginning and after the half-loading time, it falls suddenly for the remaining loading duration. This further indicates that composite materials gains strength during the initial loading condition and after wards undergo a brittle failure. This process is clearly indicated in the specimens with slow loading rates confirming that AE performs better at lower loading rates.

# Chapter 5.

# Conclusions and scope for further study

## 5.1. Conclusion

In this study, different types of materials such as mild steel, concrete and FRP composites were successfully monitored using acoustic emission technique under different types of loading. Following conclusions are made:

1. Acoustic emission technique can successfully track the damage progression in all three materials viz., Mild steel, concrete and FRP composites.
2. The amplitude of recorded AE hits exhibited a distinct behavior of damage progression in the materials. In case of mild steel, the value of amplitude ranging between 45 -100 dB were recorded during the yielding time from the load-time plot. In case of concrete, the value of amplitude increased gradually with increasing loading, wherein the maximum range from 45 to 100 dB was recorded in the last stages of loading where specimen was about to fail. However, in case of composites, it was only after half-loading time, the higher values in amplitude were recorded.
3. The analysis of distribution of AE signal amplitudes by means of Ib-values clearly indicated the severity of damage in the material with increasing loading. In case of mild steel, the lowest Ib-value was recorded during the yielding, whereas in case of concrete, the lowest values were recorded initially where load time changes slope and near failure. In case of FRP, the lowest Ib-value is recorded near the failure only.
4. The distinct Ib-vlaue plots distinguish the damage progression in all three different kind of materials. In case of mild steel, there is a single drop in plot during the yielding of the material indicating that maximum damage occurs during the yielding region. In case of concrete, the Ib-value falls for the entire duration of the loading, indicating progressive damage leading to failure. In case of FRP composites, the Ib-value exhibited a drop only after half loading time indicting the severe damage begins only after FRP is loaded to some extent.

5. From Ib-value plot and the amplitude of AE hits, it can be observed that better results are obtained when the specimens were loaded at slower rates. This was observed for all kinds of materials (mild steel, concrete and FRP composites).

## 5.2. Future Scope

1) This study could be extended to real time monitoring of bigger structures made with different materials and consequently, prediction models for damage intensity could be made.
2) This technique can be utilized with other non-destructive techniques such as ultrasonic guided waves, infra-red tomography etc. for better monitoring of structures.
3) Instead of continuous loading, AE testing could be done using cyclic loading to understand the behavior of materials.
4) A new AE setup with installed Ib value algorithm to calculate Ib values can be made so that the need of calculating Ib value from the voluminous data can be avoided.

# References


[1] R.K. Miller (Ed.), *Nondestructive Testing Handbook*. American Society for non-destructive Testing, Columbus, OH, 1987.

[2] S. Gholizadeh, "A review review of of non-destructive non-destructive testing methods of composite materials," *Procedia Structural Integrity*, vol. 1, pp. 50–57, 2016.

[3] W. J. Staszewski, S. Mahzan, and R. Traynor, "Health monitoring of aerospace composite structures – Active and passive approach," *Composites Science and Technology*, vol. 69, no. 11–12, pp. 1678–1685, 2009.

[4] R.D.Finlayson. *Handbook of nondestructive evaluation*. New York: McGraw Hill 2000.

[5] D. Karaduman, D. A. Bircan, A. Çetin, "Non-Destructive examination of underground pressure vessels using acoustic emission ( AE ) techniques ," vol. 1, no. 1, pp. 1–8, 2017.

[6] C. B. Scruby, "An introduction to acoustic emission," *J. Phys. E.*, vol. 20, no. 8, pp. 946–953, 1987.

[7] M. Ohtsu, "The history and development of acoustic emission in concrete engineering," *Magazine of Concrete Research*, vol. 48, no. 177, pp. 321-330, 1996.

[8] M. R. Kaphle, A. Tan, D. Thambiratnam, T. H. T. Chan, "Damage quantification techniques in acoustic emission monitoring," *QUT ePrints*, 2011

[9] S. Colombo, S. Colombo, I. G. Main, I. G. Main, M. C. Forde, M. C. Forde, "Assessing Damage of Reinforced Concrete Beam Using '"b -value"' Analysis of Acoustic Emission Signals," *Journal of materials in civil engineering*, vol. 15, no. 15, pp. 280–286, 2003.

[10] R. D. Finlayson, M. Friesel, M. Carlos, P. Cole, J. C. Lenain, "Health monitoring of aerospace structures with acoustic emission and acousto-ultrasonics," *Insight* , vol. 43, no. 3, pp. 155–158, 2001.

[11] K. Wang, G. Reif, S. Oh, "In-process quality detection of friction welds using acoustic emission techniques.," *Weld. J.*, no. September, pp. 312–316, 1982.

[12] G. Drummond, J. F. Watson, P. P. Acarnley, "Acoustic emission from wire ropes during proof load and fatigue testing," *NDT&E International* , vol. 40, no. 1, pp. 94–101, 2007.

[13] J. H. Kurz, F. Fink, C. U. Grosse, H. Reinhardt, “Stress Drop and Stress Redistribution in Concrete Quantified Over Time by the b-value Analysis,” *Structural Health Monitoring*, vol. 5, no. 1, pp. 69–81, 2006.

[14] T. H. Loutas, G. Sotiriades, I. Kalaitzoglou, V. Kostopoulos, “Condition monitoring of a single-stage gearbox with artificially induced gear cracks utilizing on-line vibration and acoustic emission measurements,” *Applied Acoustics*, vol. 70, no. 9, pp. 1148–1159, 2009.

[15] E. Proverbio, V. Venturi, G. Campanella, “Damage assessment in post-tensioned concrete viaduct by,” *Non-Destructive Testing in Civil Engineering*, 2009.

[16] T. Haneef, B. Lahiri, S. Bagavathiappan, C. K. Mukhopadhyay, J. Philip, B. P. C. Rao, T. Jayakumar “Study of the tensile behavior of AISI type 316 stainless steel using acoustic emission and infrared thermography techniques,” *J. Mater Res Technol.*, vol. 4, no. 3, pp. 241–253, 2015.

[17] A. Mostafapour S. Davoodi, “A theoretical and experimental study on acoustic signals caused by leakage in buried gas-filled pipe,” *Applied Acoustics*, vol. 87, pp. 1–8, 2015.

[18] R. Vidya Sagar, M. V. M. S. Rao, “An experimental study on loading rate effect on acoustic emission based b-values related to reinforced concrete fracture,” *Construction and Building Materials*, vol. 70, pp. 460–472, 2014.

[19] Z. Chen, D. Li, Y. Li, Q. Feng, “Damage analysis of FRP/steel composite plates using acoustic emission,” *Pacific Science Review*, vol. 16, no. 3, pp. 193–200, 2014.

[20] T. Chuluunbat, C. Lu, A. Kostryzhev, A. K. Tieu, “Influence of loading conditions during tensile testing on acoustic emission,” Key Engineering Materials, vol. 6, pp. 121-126, 2015.

[21] P. R. Prem, A. R. Murthy, “Acoustic emission monitoring of reinforced concrete beams subjected to four-point-bending,” *Applied Acoustics*, 2016.

[22] M. Shigeishi, S. Colombo, K. J. Broughton, H. Rutledge, A. J. Batchelor, “Acoustic emission to assess and monitor the integrity of bridges,” *Construction and Building Materials*, no. 15, pp. 35–49, 2001.

[23] M. Wevers, K. Lambrighs, “Applications of Acoustic Emission for SHM : A Review,” *Encyclopedia of Structural Health Monitoring*, pp. 1–13, 2009.

[24] A.A.Pollock, “Acoustic Emission Inspection”, *Princeton Junction*, NJ; 1989.

[25] “ ASTM A370. Standard Test Methods and Definitions for Mechanical Testing of Steel Products”, American Society for Testing of Materials, 2003.

[26] “ASTM D3039. Standard test method for tensile properties of polymer matrix composite materials”, American Society for Testing of Materials, 2014.

# Web References


[W1] "Acoustic Emission (AE) Technology," *Acoustic Emission Systems and NDT Products by PHYSICAL ACOUSTICS*. [Online]. Available: http://www.physicalacoustics.com/ae-technology/. [Accessed: 20-Mar-2017].

[W2] "Acoustic Emission Testing," *Acoustic Emission Testing*. [Online]. Available: https://www.nde-ed.org/EducationResources/CommunityCollege/Other%20Methods/AE/AE_Equipment.php. [Accessed: 25-Mar-2017].

# ANNEXURE

- **Flowchart of matlab code for Ib-value analysis**